Transcriptomic analysis of adult mouse cardiac stromal cells using single-cell qRT-PCR

Rita Alonaizan[1,2,3], Patricia Chaves-Guerrero[4], Sara Samari[4], Michela Noseda[4], Nicola Smart[1,2], Carolyn Carr[1]

1 Department of Physiology, Anatomy & Genetics, University of Oxford, Oxford, UK.
2 Institute of Developmental and Regenerative Medicine, Old Road Campus, University of Oxford, Oxford, UK.
3 King Faisal Specialist Hospital & Research Centre, Riyadh, Saudi Arabia.
4 National Heart and Lung Institute, Imperial College London, London, UK.

Correspondence: rita.alonaizan@dpag.ox.ac.uk

Keywords: heart regeneration, cell therapy, cardiosphere-derived cells, cardiac progenitor cells, myocardial infarction, single-cell qRT-PCR.

Abstract

Fate mapping studies have challenged the longstanding view of the adult mammalian heart as a post-mitotic organ, suggesting limited cardiomyocyte renewal. This has spurred efforts to identify cardiac progenitor cell (CPC) populations, but their contribution to cardiac regeneration has been found to be minimal compared to cardiomyocyte proliferation. Despite this, CPC transplantation has shown therapeutic potential through paracrine signalling.

The identity of CPCs remains unclear due to overlapping characteristics with other cardiac stromal cell populations such as fibroblasts, mesenchymal cells, and pericytes. This study sought to optimise the isolation of CPCs by developing a cardiac collagenase-trypsin (CT) protocol, which was compared to the established method of isolating cardiosphere-derived cells (CDCs). The CT protocol resulted in a higher cell yield and reduced expansion time, with both CTs and CDCs showing superior survival potential under serum starvation compared to commercially acquired cardiac fibroblasts (CFs).

Single-cell qRT-PCR analysis revealed that CTs and CDCs share a similar gene expression profile, distinct from CFs, characterised by the enrichment of cardiogenic transcription factors. Notably, CTs exhibited higher expression of *Tcf21* and lower *Tbx5*, suggesting an epicardial-derived fibroblast phenotype, whereas *Tbx5* was enriched in CDCs and CFs. Additionally, CTs showed an enrichment of macrophage-associated genes *Mrc1* and *Csf1r*, possibly due to the transdifferentiation of macrophages to or from a fibroblast phenotype in a subset of CTs. The study concludes that CTs represent a robust and efficient source of CPCs with therapeutic potential and offers insights into the complex identity of cardiac stromal cells.

Introduction

Evidence stemming from fate mapping studies of cardiomyocyte renewal in the adult mammalian heart challenged the dogma considering the heart as a post-mitotic organ[1-3]. Therefore, multiple research groups attempted to characterise endogenous cardiac populations that may have a role in the regenerative process. Identifiers of the presumed cardiac progenitor cell (CPC) populations include SCA1 and the SP dye-efflux phenotype, KIT, ISL1, cardiosphere- and colony-forming assays, or re-activation of the embryonic epicardial programme and WT1 upregulation[4]. More recent findings indicate that the mechanism behind cardiomyocyte renewal is cardiomyocyte proliferation, and that CPC contribution is minimal[1-6]. Despite their low cardiomyogenic potential after transplantation into the infarcted heart, CPCs have demonstrated therapeutic benefits in pre-clinical studies, primarily due to paracrine signalling[7-11].

The identity of CPCs remains unclear, with numerous studies questioning the distinctions between CPCs and various cardiac stromal cell populations, including mesenchymal cells, fibroblasts, and pericytes[12-16]. This uncertainty stems from the overlap in their morphology and gene expression profiles. For instance, cardiac fibroblasts, like CPCs, express cardiogenic transcription factors that contribute to cardiac development and repair[17]. Both cardiac and tail fibroblasts share a molecular signature similar to that of mesenchymal stem cells (MSCs)[18]. Significant efforts have been made to distinguish these cardiac stromal cells. To complicate matters further, single-cell transcriptional profiling of mouse ventricular non-myocytes has revealed subpopulation heterogeneity within the cardiac fibroblast population[19]. Additionally, markers commonly used to identify pericytes are relatively non-specific, albeit some genes are enriched in pericytes compared to other cell types[19].

Certain research groups have sorted CPCs based on surface marker expression followed by clonogenic selection, which include the derivation of SCA1+ PDGFRα+/SP cells[9,20]. These methods produced homogeneous, self-renewing cardiogenic populations that showed promise. However, these cell types are found at very low rates in the adult mouse heart, with a reported cloning efficiency of around 1-2%. Ideally, an optimal cell isolation protocol would yield a large, robust, and reproducible population of cells in the shortest possible duration. The isolation of cardiosphere-derived cells (CDCs) involves culturing cardiac explants to harvest explant-derived cells (EDCs), which are then induced to form cardiospheres. EDCs vary in morphology and time required to achieve confluent culture, with CDC expansion times ranging from 5 to 84 days[21].

To optimise CPC isolation, we developed a cardiac collagenase-trypsin (CT) protocol adapted from studies by Gharaibeh *et al*.[22] and Okada *et al*.[23] for isolating slowly adhering cells (SACs) from skeletal muscle. These SACs demonstrated superior differentiation, survival, and therapeutic potential compared to rapidly adhering cells (RACs). Comparably, we showed that these CPCs, which we term CTs, can be induced to differentiate into the cardiomyocyte lineage *in vitro*[24] using TGFβ1 stimulation[25,26]. We also showed that fatty acid supplementation triggered a metabolic switch via the PPARα pathway, evidenced by upregulated oxidative metabolism and increased expression of cardiomyocyte markers in CTs[24]. This aligns with the metabolic switch from glycolysis to fatty acid oxidation observed during cardiomyocyte maturation in development[27]. In this study, we characterise the presumed CPC populations, CTs and CDCs, in comparison to commercially acquired primary cardiac fibroblasts (CFs) (**Figure 1**) using single-cell qRT-PCR and cell survival assays. Our aim is to profile CPCs obtained without clonogenic and marker selection and compare them to the cardiac fibroblast compartment.

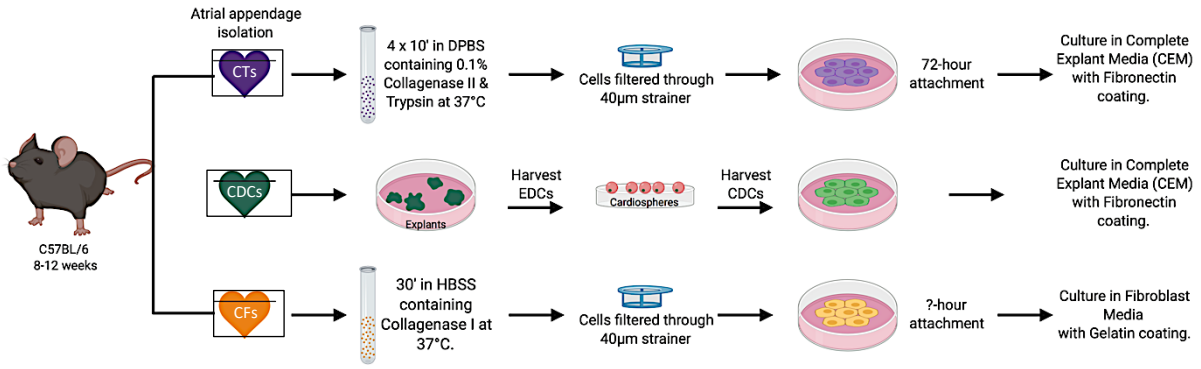

Figure 1. Isolation method of the three cardiac stromal populations, CTs, CDCs and CFs. *Schematic showing the protocol used to isolate CTs, CDCs, and CFs. The isolation protocol of CTs and CDCs is detailed in the Methods. As CFs were purchased and not isolated in our lab, some information is lacking e.g. age of mice, duration of cell attachment, and composition of the accompanying media. Illustration created with BioRender.com.*

Results

The CT protocol produces higher cell yield compared to CDCs, but a similar survival potential.

CTs and CDCs were isolated from adult mouse atrial tissue and expanded for further analysis. The average time to reach 90% confluency at passage 0 and passage 1 was considerably shorter for CTs, taking approximately 10 days and 20 days, respectively. In contrast, CDCs required around 40 days to passage 0 and 60 days to passage 1, due to the additional steps involved in explant culture and cardiosphere formation (**Figure 2.A**).

After expansion to passage 3, we assessed the survival potential of CTs compared to CDCs and commercially acquired CFs to determine their robustness for transplantation. Serum starvation was used to challenge the cells in culture for 3 days and 10 days. CTs, CDCs, and CFs continued to grow following serum starvation with no significant difference in cell numbers detected at day 3. At day 10, CT cell numbers were significantly higher than CFs but not CDCs, suggesting that CTs have a superior survival potential compared to CFs (**Figure 2.B**).

Single-cell profiling of cardiac stromal cells.

CTs, CDCs and CFs isolated from adult mouse atrial tissue were expanded to passage 3 for single-cell qRT-PCR analysis and compared with the HL-1 cardiomyocyte line which was used as a control (**Figure 3**). Genes selected for this experiment (detailed in supplementary table 1) included those encoding cardiogenic transcription factors, stem cell-related markers, fibroblasts, cardiomyocytes and other genes that were differentially expressed in the SCA1 subpopulations according to the Noseda *et al*. study[9]. Moreover, we attempted to detect different cardiac subpopulations including pericytes, endothelial cells and macrophages within the cardiac stromal cell populations. The heatmap (**Figure 3.A**) shows that the HL-1 cardiomyocytes were distinct from the cardiac stromal cells with expression of each gene across the different populations shown in **Figure 3.B**. The cardiac stromal populations expressed the fibroblast-associated genes *Cd44*, *Ddr2*, *Pdgfrb*, *Acta2* (encodes αSMA), and *Vim*, albeit CFs had less consistent expression of *Pdgfrb*, and *Acta2*. Interestingly, *Ddr2, Acta2* and *Vim* were also expressed by HL-1 cardiomyocytes. Additionally, on rare occasions, CFs (n=2/29) and CTs (n=3/55) co-expressing *Wt1* and *Tcf21* were detected, perhaps inferring an epicardial-derived fibroblast identity. *Ly6a* (encodes SCA1) and *Pdgfra* were expressed in all three populations. The three cardiac stromal populations expressed little or no *Prg4* and *Wif1* but displayed expression of *Medag* and *Col1a1*. *Ms4a4d* expression was detected in CTs and some CFs only. Regarding pericyte-associated markers, *Kcnj8* showed little or no expression in all populations, *Colec11* showed sporadic expression, whereas *Ng2* showed high expression in all three cardiac stromal populations.

In CTs and CDCs, the most prevalent cardiogenic transcription factors were *Gata4*, *Tbx20*, *Hand2*, and *Mef2a* with little or no expression of *Hand1*, *Isl1*, and *Nkx2-5*. In contrast, CFs had less uniform expression of *Gata4*, *Tbx20*, and *Hand2*. Unlike CDCs, both CTs and CFs expressed *Mef2c* heterogeneously. The expression of *Tbx5* in CFs followed a similar pattern to CDCs but was more sporadic in CTs. Interestingly, only CFs expressed *Isl1,* which has a very limited expression profile in the adult heart[28,29]. The three cardiac stromal populations had very little or no expression of markers of cardiomyocytes (*Nppa*, *Myh6*, and *Myl2*), haematopoietic (*Cd45*) and endothelial cells (*Cdh5* and *Vwf*), except for *Kdr* expression, which was detected in the CTs, CFs and HL-1 cardiomyocytes. Expression of stem cell-related markers (*Pou5f1*, *Nanog*, *Klf4*, and *Tert*) was found in the three cardiac stromal populations. *Pou5f1*, *Nanog*, and *Klf4*, but not *Tert*, were also expressed in HL-1 cardiomyocytes. As expected, HL-1 cardiomyocytes had a distinctly different expression profile and displayed expression of most cardiogenic transcription factors (*Gata4*, *Hand2*, *Mef2a/c*, *Nkx2-5* and *Tbx5/20*), and cardiomyocyte markers (*Nppa*, *Myh6*, and *Myl2*).

Expression of Schwann cell-related markers (*Plp1* and *Kcna1*) was found sporadically in all populations, except for HL-1 cardiomyocytes where only *Plp1*, but not *Kcna1*, was expressed. We also assessed the expression of the macrophage-associated genes *Mrc1*, *Csf1r* and *Cx3cr1*. *Cx3cr1* showed no expression in any population, and *Mrc1* was only expressed in CTs. In contrast, *Csf1r* was expressed in all three stromal populations but showed a more uniform pattern in CTs.

A comparison of the molecular profiles of CPCs and CFs.

By principal component analysis (PCA), cardiac stromal cells and HL-1 cardiomyocytes were resolved as discrete groups, which is consistent with their distinct phenotypes. Gene loadings contributing to each dimension (Dim) suggest that a small subset of genes explain the cross-group variability captured by Dim.1 and Dim.2. The separation of HL-1 cardiomyocytes was attributable to *Wif1*, *Nkx2-5*, *Mef2c*, *Nppa*, *Myl2*, and *Myh6* (**Figure 4.A**). Some separation of CFs from CTs was also revealed, with the CDCs clustering between the other two populations. This can be seen more clearly in the PCA of the stromal populations alone (**Figure 4.B**). The separation of CTs was attributable to *Tcf21*, clearly seen in **Figure 4.B**, while the separation of CDCs and CFs was mainly attributable to *Tbx5*. This *Tcf21* versus *Tbx5* polarity may reflect functional or origin heterogeneity. CFs appeared more dispersed, suggesting higher heterogeneity, in comparison to CTs and CDCs, which again is more apparent in the PCA of stromal populations only.

Statistical analysis comparing the three cardiac stromal population revealed that CTs were more similar to CDCs than CFs with CTs showing significantly higher expression of *Vim* ($P < 0.05$), *Kdr* ($P < 0.05$), *Mrc1* ($P < 0.001$), *Tcf21* ($P < 0.0001$), *Ms4a4d* ($P < 0.0001$), *Tbx20* ($P < 0.0001$), *Csf1r* ($P < 0.0001$), *Mef2c* ($P < 0.0001$), and *Medag* ($P < 0.05$), but lower expression of *Tbx5* ($P < 0.0001$) and *Acta2* ($P < 0.01$), compared to CDCs. In comparison to the CFs, CTs showed significantly higher expression of *Col1a1* ($P < 0.0001$), *Pdgfrb* ($P < 0.0001$), *Hand2* ($P < 0.0001$), *Pou5f1* ($P < 0.05$), *Mrc1* ($P < 0.001$), *Tcf21* ($P < 0.0001$), *Tbx20* ($P < 0.0001$), *Ng2* ($P < 0.01$), *Mef2c* ($P < 0.05$), *Medag* ($P < 0.001$), and *Gata4* ($P < 0.0001$), but lower expression of *Isl1* ($P < 0.0001$) and *Tbx5* ($P < 0.01$) (**Figure 5.A**).

Finally, we performed co-expression correlation to further support the inferred biological functions of the stromal and cardiomyocyte populations (**Figure 5.B**). Correlation plot analysis showed a polarisation between the expression of some fibroblast-associated markers and cardiogenic transcription factors, and a positive correlation between the expression of cardiogenic transcription factors and cardiomyocyte markers. *Tcf21* expression showed a positive correlation with the expression of *Tbx20*, *Ms4a4d,* and macrophage-associated genes *Csf1r* and *Mrc1*. This is attributed to the high co-expression of these genes in CTs. In addition, expression of pericyte-associated gene *Kcnj8* showed a positive correlation with the expression of *Isl1* due to their co-expression pattern in a small number of CFs. Collectively, these data confirm the co-expression of cardiogenic markers, associated predominantly with CTs and CDCs, as distinct from the gene profile that characterises CFs. Additionally, the enrichment of *Tcf21* expression in CTs further delineates CTs from CFs.

A

	Average time to 90% confluency at P0	Average time to 90% confluency at P1
CDCs	40 days	60 days
CTs	10 days	20 days

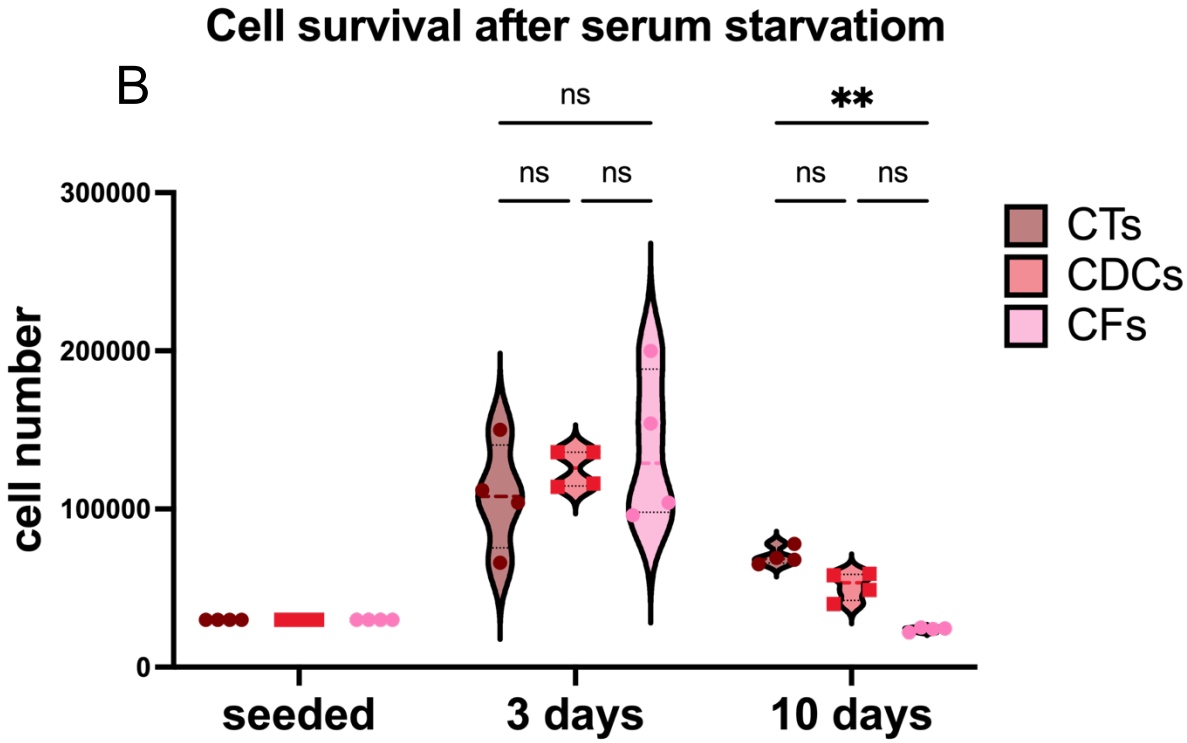

Figure 2. **The CT protocol produces higher cell yield compared to CDCs but a similar survival potential.** ***(A)*** *Average time to reach 90% at passage 0 and passage 1, as assessed by cell counting, in CTs and CDCs.* ***(B)*** *Cell Survival following serum starvation for 3 or 10 days, as assessed by cell counting, in CTs, CDCs and CFs. Analysed using a two-way ANOVA with Tukey's multiple comparisons test to determine statistical significance (n=4), * $p < 0.05$, ** $p < 0.01$.*

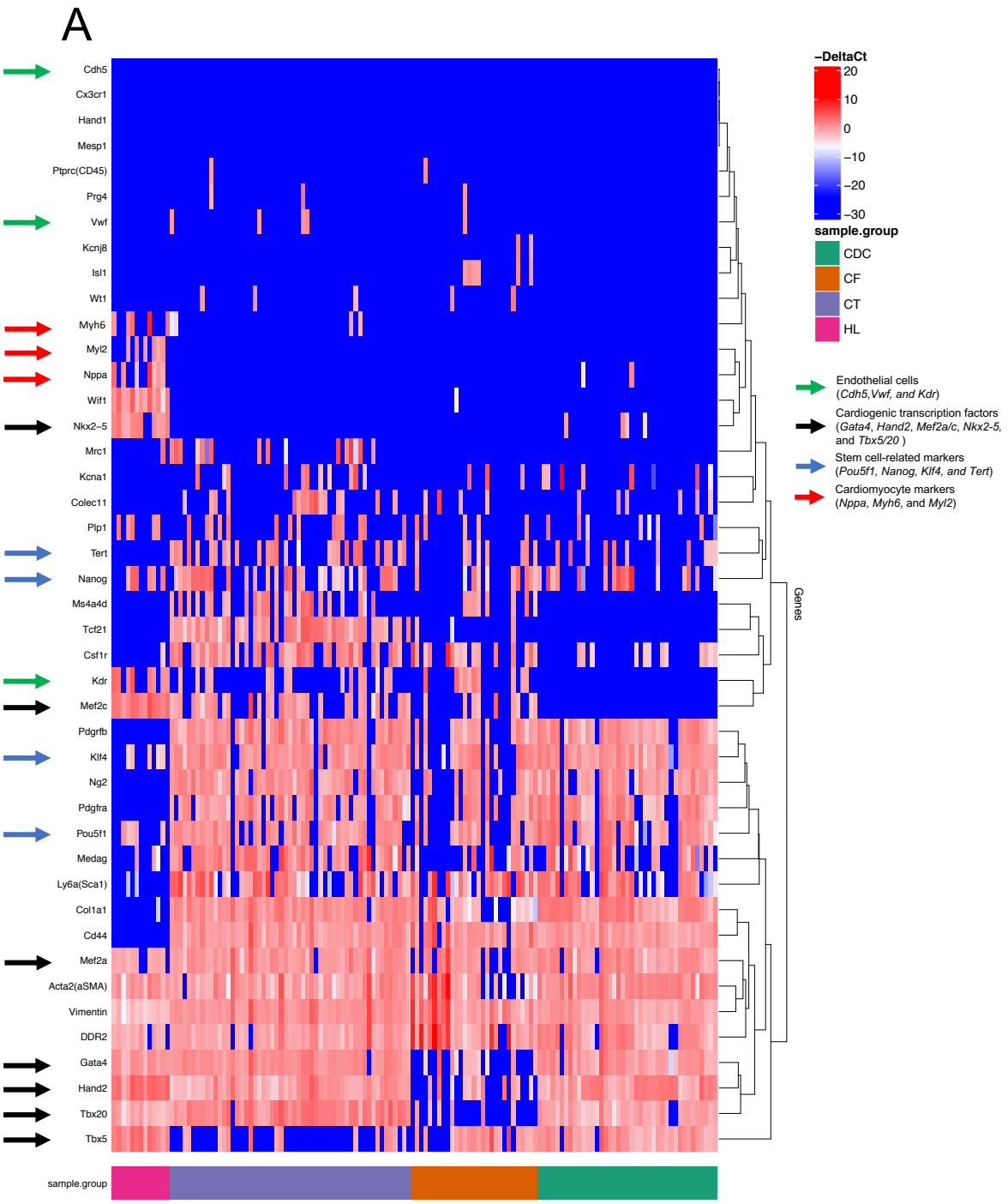

Figure 3. Single-cell analysis reveals an enrichment of Tcf21 and low expression of Tbx5 in CTs, compared to CDCs and CFs. (A) *Expression of 43 genes was analysed at the single-cell level in the four cell populations shown: CTs (n=55), CDCs (n=41) and CFs (n=29) at passage 3, in addition to HL-1 cardiomyocytes (n=13). Both CTs and CDCs represent 3 biological replicates. The heatmap illustrates expression as -ΔCT values (blue is low or absent; red is high). Samples were ordered based on cell type, and the genes grouped by a hierarchical clustering algorithm based on the underlying co-expression pattern.* ***(B)*** *Single-cell expression of the 43 genes tested, represented individually in the four cell populations shown with the mean represented as a black diamond in each set.*

B

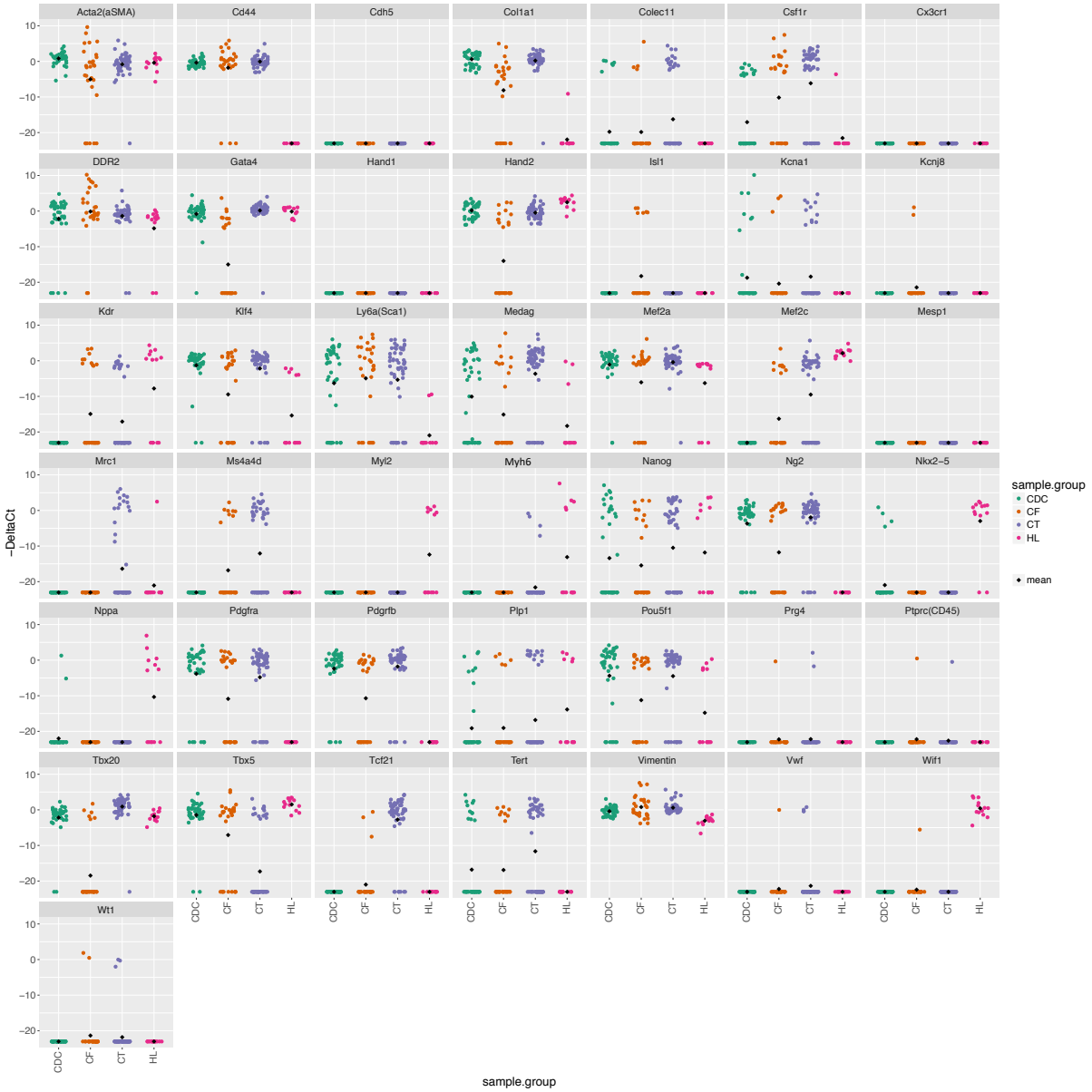
Acta2(aSMA)
Cd44
Cdh5
Col1a1
Colec11
Csf1r
Cx3cr1
DDR2
Gata4
Hand1
Hand2
Isl1
Kcna1
Kcnj8
Kdr
Klf4
Ly6a(Sca1)
Medag
Mef2a
Mef2c
Mesp1
Mrc1
Ms4a4d
Myl2
Myh6
Nanog
Ng2
Nkx2−5
Nppa
Pdgfra
Pdgrfb
Plp1
Pou5f1
Prg4
Ptprc(CD45)
Tbx20
Tbx5
Tcf21
Tert
Vimentin
Vwf
Wif1
Wt1
−DeltaCt
10
0
−10
−20
CDC
CF
CT
HL
sample.group
sample.group
CDC
CF
CT
HL
mean

194

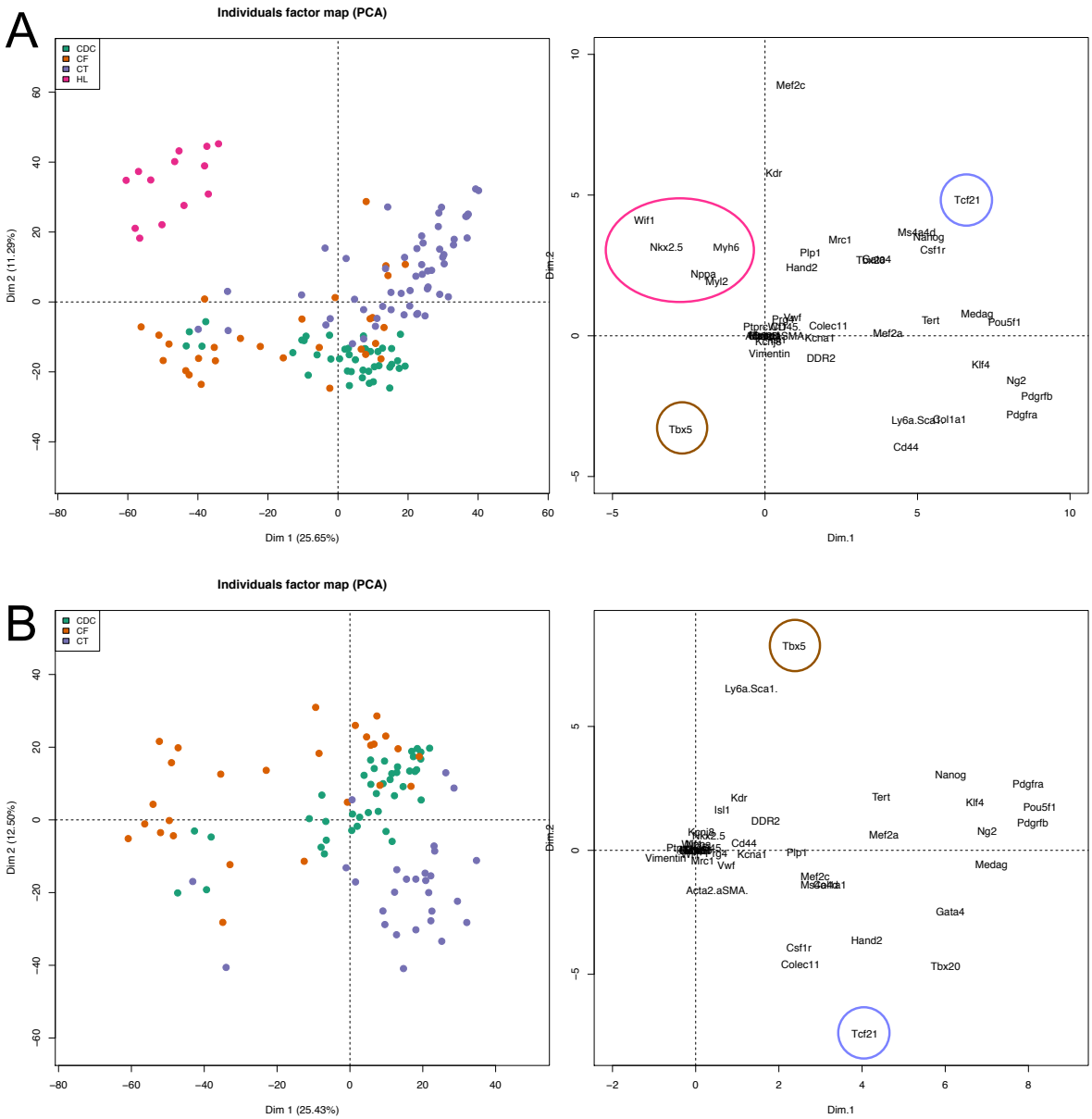

Figure 4. PCA of the three cardiac stromal populations and HL-1 cardiomyocytes. (A) *PCA of the four cell populations shown: CTs (n=55), CDCs (n=41) and CFs (n=29) at passage 3, in addition to HL-1 cardiomyocytes (n=13). Both CTs and CDCs represent 3 biological replicates. Dim.1 separates the cardiac stromal populations, whereas Dim.2 shows a distinct separation between cardiac stromal and myocyte populations. Gene loadings contributing to each Dim suggest that a small subset of genes explain the cross-group variability captured by Dim.1 and Dim.2. Tcf21 is associated with CTs (emphasised in the blue circle), whereas Tbx5 is associated with CDCs and CFs (emphasised in the brown circle). The separation between cardiac stromal and myocyte populations is reflected by clustering of cardiogenic and cardiomyocyte genes (Nkx2.5, Wif1, Nppa, Myl2 and Myh6), which are emphasised in the pink circle.* ***(B)*** *PCA of the three cardiac stromal populations alone: CTs (n=28), CDCs (n=41), CFs (n=27). Both CTs and CDCs represent 3 biological replicates. Gene loadings contributing to each Dim show that Tcf21 is associated with CTs, whereas Tbx5 is associated with CDCs and CFs.*

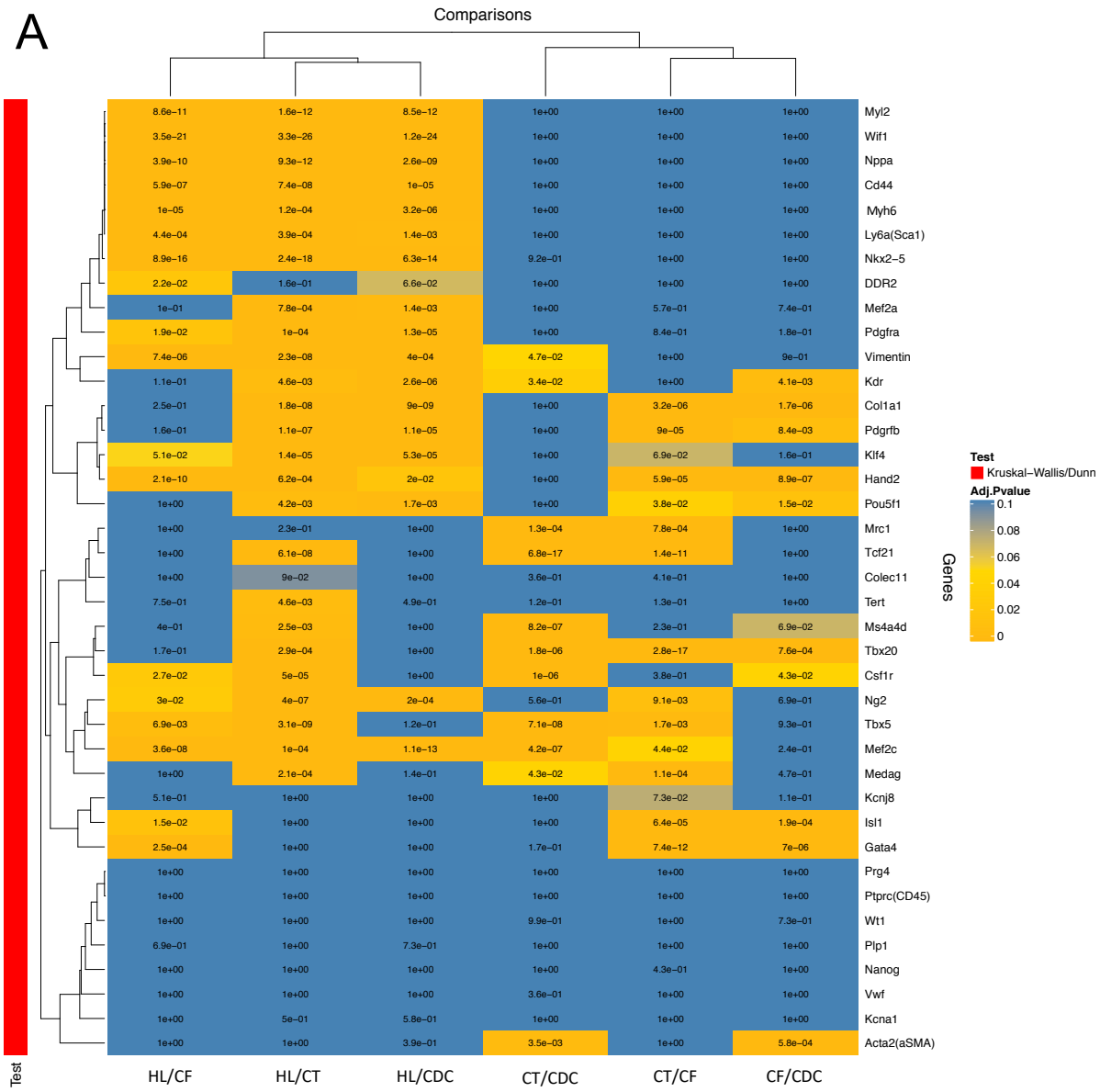

Figure 5. Statistical analysis of the single-cell qRT-PCR and gene correlations. ***(A)*** *Statistical analysis of the four cell populations shown: CTs (n=55), CDCs (n=41) and CFs (n=29) at passage 3, in addition to HL-1 cardiomyocytes (n=13). Both CTs and CDCs represent 3 biological replicates. The heatmap illustrates P values from 0 to 0.1 (orange to blue is low to high). The genes were grouped by a hierarchical clustering algorithm based on the underlying co-expression pattern.* ***(B)*** *Gene correlation plot, derived from the single-cell qRT-PCR data, is represented by the colour of the dots (blue is negative; red is positive). Both the diameter and colour intensity of each dot are proportional to the level of correlation.*

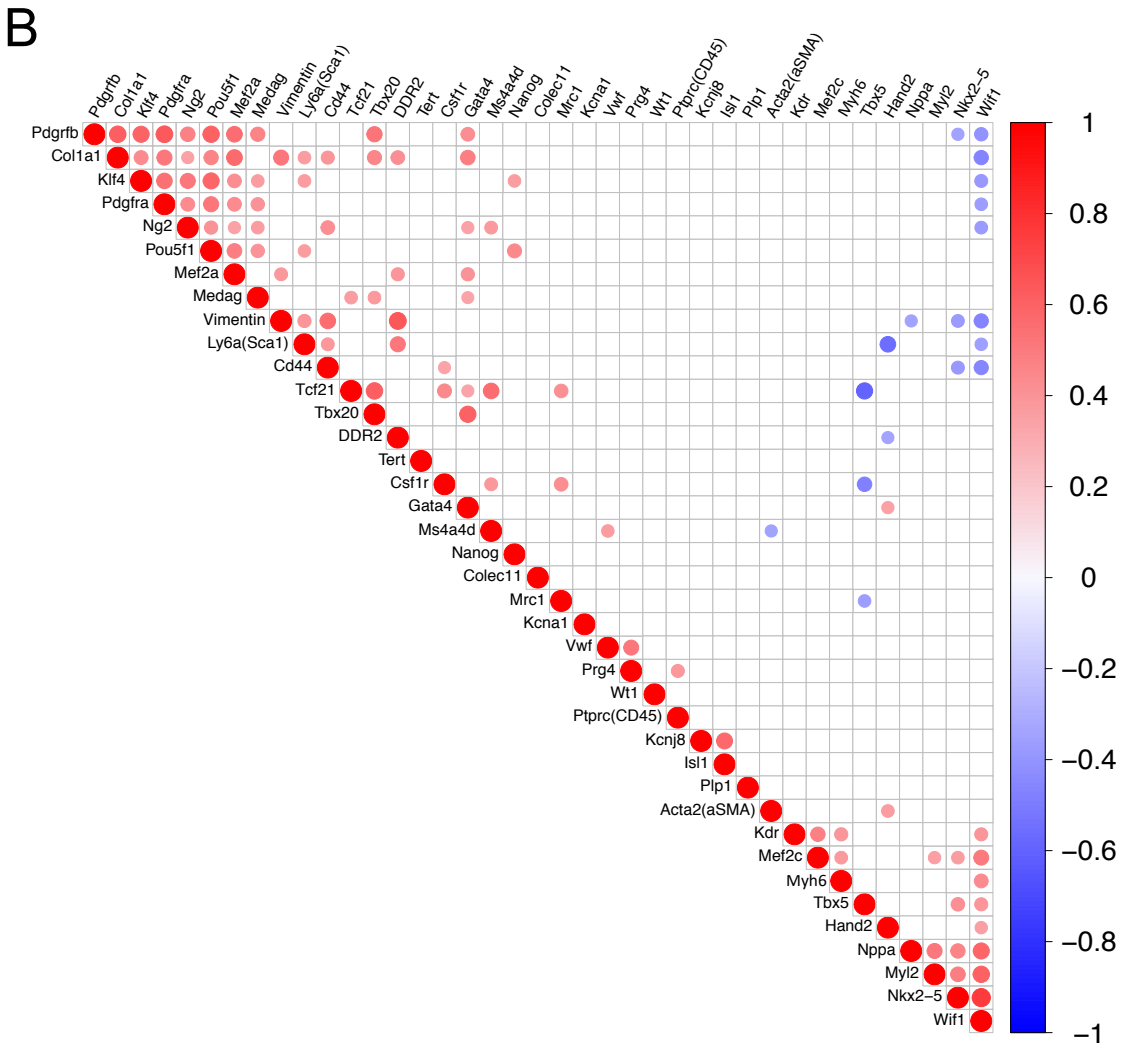
B
Pdgrfb
Col1a1
Klf4
Pdgfra
Ng2
Pou5f1
Mef2a
Medag
Vimentin
Ly6a(Sca1)
Cd44
Tcf21
Tbx20
DDR2
Tert
Csf1r
Gata4
Ms4a4d
Nanog
Colec11
Mrc1
Kcna1
Vwf
Prg4
Wt1
Ptprc(CD45)
Kcnj8
Isl1
Plp1
Acta2(aSMA)
Kdr
Mef2c
Myh6
Tbx5
Hand2
Nppa
Myl2
Nkx2−5
Wif1
1
0.8
0.6
0.4
0.2
0
−0.2
−0.4
−0.6
−0.8
−1

219

Discussion

CTs have reduced expansion time and a superior survival potential following serum starvation.

Low survival and retention of transplanted cells following ischaemic events is mainly due to the harsh conditions within the infarct region that include hypoxia, inflammation, and nutrient restriction. Serum in cell culture media provides amino and fatty acids and its withdrawal is therefore, considered a form of nutrient restriction and serum starvation is an effective way of inducing cell apoptosis[30]. Here, we found that all three cardiac stromal populations continued to grow following serum starvation with no significant difference in cell numbers detected at day 3. However, CF cell numbers at day 10 were similar to the cell number seeded initially suggesting substantial cell death. At day 10, CT cell numbers were significantly higher than CFs but not CDCs, suggesting that CTs have a superior survival potential to that of CFs. This is consistent with the single-cell qRT-PCR results showing that CTs and CDCs share a more similar gene expression profile in comparison to the CFs. Tolerance to serum starvation has also been observed in MSCs under both normoxic and hypoxic culture conditions[31,32].

Reduced robustness was noticed during routine culture of CFs in comparison to CTs and CDCs as shown by increased time to reach confluency and higher numbers of floating dead cells in culture (data not shown). The CFs displayed reduced recovery following single-cell sorting for the single-cell qRT-PCR experiment, in comparison to CTs and CDCs. It is difficult to pinpoint what is responsible for this fragility due to difference in gene expression, cell culture media and coating substrate. Differential effects of various culture coating substrate types on cell proliferation have been shown[33]. However, standardising the culture conditions of all cell types would have been counterproductive as our aim was to compare the populations as they would be cultured in other labs based on their recommended and published culture conditions. Ideally, the survival potential of these different stromal population should be compared following transplantation into infarcted hearts or in *in vitro* conditions that more closely mimic the *in vivo* environment following MI. Overall, our data suggested that CTs and CDCs were more robust than CFs, both in long-term cell expansion and survival under serum starvation. The survival potential of cardiac stromal populations may differ in response to stress *in vitro*, which can be an indication of their *in vivo* behaviour following transplantation. Additionally, the reduced expansion time needed to generate CTs, compared to CDCs, indicated that a CDC-like population for therapeutic use could be achieved more efficiently.

CPCs show a fibroblast phenotype with no detection of endothelial cells or pericytes.

A study by Skelly *et al*. 2018 examined the single-cell transcriptional profile of adult mouse ventricular nonmyocytes to identify distinct cell populations[19]. Subpopulation heterogeneity within the cardiac fibroblast population was described where most fibroblasts "fibroblasts 1" were characterised by high expression of *Medag, Ms4a4d, Pdgfra* and *Tcf21*, while a smaller distinct cluster "fibroblasts 2" expressed higher levels of *Tbx20*, *Wif1* and *Prg4*. Although we found that *Tbx20* was highly expressed in both CTs and CDCs, *Wif1* and *Prg4* showed little to no expression in all stromal populations. Moreover, *Medag* and *Pdgfra* expression was detected in all three populations, whereas *Ms4a4d* and *Tcf21* was only found in CTs and CFs. However, CFs showed less consistent expression of *Ms4a4d* compared to CTs. This suggests that none of the three stromal populations fit the expression pattern of "fibroblasts 2" and that CTs were the best match to the expression pattern of "fibroblasts 1". However, an important consideration to make is that the study by Skelly *et al*. examined ventricular rather than atrial nonmyocytes and used freshly isolated cells rather than passaged cells which may undergo phenotypic drift *in vitro*.

Additional mesenchymal- and fibroblast-associated genes were assessed including *Vim*, *Ddr2*, *Acta2*, *Cd44*, and *Col1a1*. αSMA, encoded by *Acta2,* is a protein commonly used to identify smooth muscle cells, pericytes and myofibroblasts, which acquire a contractile phenotype similar to that of smooth muscle cells upon differentiation[34]. *Vim* was the only gene

271 expressed in all the screened cells of all populations. Vimentin is an intermediate filament
272 protein that has been widely used as a reliable marker of mesenchymal cells, highly migratory
273 cells derived by EMT, and has a protective role against nuclear rupture and DNA damage
274 during migration[35]. None of these markers showed specificity to a certain population. *Vim*,
275 *Ddr2* and *Acta2* were also expressed in HL-1 cardiomyocytes, an adult immortalised atrial cell
276 line that has been shown to be similar to a mitotic embryonic cardiomyocyte rather than a
277 mature adult cell[36], as reflected by their immature energy metabolism[37]. The expression of
278 mesenchymal- and fibroblast-associated genes in HL-1 cardiomyocytes may reflect the lack
279 of specificity of these markers in *in vitro* cultures, the immature phenotype of HL-1
280 cardiomyocytes and/or their dedifferentiation in culture. Genomic instability is a common
281 setback associated with the use of cell lines in research[38]. Nonetheless, the above data
282 suggest a fibroblast-like phenotype of all stromal populations. A combination of *Pdgfra, Col1a1*
283 *and Medag,* which were expressed in the stromal cells but not the HL-1 cells, might be more
284 reliable markers for identifying *in vitro* fibroblast cultures.

285 Commonly used markers to identify pericytes (e.g. *Pdgfrb* and *Ng2*) are relatively non-specific.
286 However, *Kcnj8* and *Colec11* have been identified as genes that show higher expression in
287 pericytes relative to other cell types expressing them[19]. We found little or no expression of
288 *Kcnj8* in any population. *Colec11* showed sporadic expression, whereas *Ng2* and *Pdgfrb*
289 showed high expression in all three cardiac stromal populations. Therefore, there is no
290 conclusive evidence to suggest that these stromal populations are pericytes in their
291 phenotype. Our data also suggest that the specificity of *Kcnj8* and *Colec11* expression to
292 pericytes might be superior to that of commonly used markers. Moreover, the expression of
293 *Kcnj8* was positively correlated with *Isl1*, attributable to co-expression in a small number of
294 CFs. ISL1-mediated differentiation of coronary pericytes to coronary artery smooth muscle
295 cells has been described in the embryonic heart[39]. Although *Isl1* expression is detected in the
296 developing heart and multipotent $ISL1^+$ progenitors play an important role in giving rise to
297 cardiac lineages during development[40], $ISL1^+$ cells are very rare in adult human and murine
298 hearts[41,42].

299 The three cardiac stromal populations had very little or no expression of markers of
300 cardiomyocytes (*Nppa*, *Myh6*, and *Myl2*), haematopoietic (*Cd45*), or endothelial cells (*Cdh5*
301 and *Vwf*). Expression of *Nppa* and *Myh6* was found in few CDCs (2 $Nppa^+$ cells, n=41) and
302 CTs (4 $Myh6^+$ cells, n=55). Given that these cells are at passage 3, it is highly unlikely that the
303 cells expressing *Nppa* or *Myh6* cells are cardiomyocytes that survived the isolation protocol.
304 This expression may be a result of spontaneous differentiation in culture or may reflect some
305 progenitor status. In addition, *Kdr* expression, a marker of endothelial cells, was detected in
306 the CTs, CFs and HL-1 cardiomyocytes. During development, KDR^+ progenitors, deriving from
307 the $MESP1^+$ mesodermal lineage, have a cardiovascular tri-lineage potential[43,44]. It has been
308 shown by lineage tracing that precursors expressing *Gata5* and *Wt1* give rise to the adult
309 $SCA1^+ SP^+$ population ($PDGFR\alpha^+/CD31^-$), whereas the adult $SCA1^+ SP^-$ population ($PDGFR\alpha^-$
310 $/CD31^+$) is mainly derived from precursors expressing *Kdr*[9]. However, CTs lack the expression
311 of other endothelial markers as observed in the $SCA1^+ SP^-$ population. *Kdr* expression has
312 also been described in coronary adventitial progenitors with cardiogenic potential[45] and in
313 endothelial progenitors[46]. Therefore, *Kdr* expression may reflect some progenitor status as
314 opposed to the presence of endothelial cells. CDCs have been examined at the single cell
315 transcriptomics level[47] and characterised as mesenchymal/stromal/fibroblast-like, with a small
316 subset of endothelial-like cells. Notably, transplantation of SCA1+ CDCs but not SCA1− CDCs
317 enhanced cardiac function after MI, highlighting the previously unappreciated functional
318 differences between CDC subpopulations.

319 A few cells co-expressing *Wt1* and *Tcf21* were detected in both the CF and CT populations.
320 In the developing heart, cells of the epicardium are identified through the expression of *Wt1*,
321 *Tbx18*, *Tcf21*, and *Raldh2*[48]. It has been demonstrated that the majority of $TCF21^+$ epicardium-
322 derived cells (EPDCs) are committed to the cardiac fibroblast lineage and that *Tcf21*

323 expression persists in cardiac fibroblasts of the adult heart[49-51]. Although WT1 is
324 downregulated following gestation[52,53], its expression is still detected in the epicardium and a
325 subset of coronary endothelial cells in the healthy adult heart[50,54]. Enrichment of the epicardial
326 markers *Wt1* and *Tcf21* has been shown in adult cardiac fibroblasts[17]. More recent studies
327 showed that *Wt1* is expressed in more cell types than previously appreciated with a study
328 describing a Wt1b$^+$ macrophage subpopulation that plays an essential role in zebrafish heart
329 and fin regeneration[55]. In our data, *Wt1* expression did not show a correlation with *Mrc1* or *Kdr*
330 but all cells expressing *Wt1* were also positive for *Tcf21* suggesting a fibroblast phenotype.

331 Expression of stem cell-related markers (*Pou5f1*, *Nanog*, *Klf4*, and *Tert*) was found in all three
332 cardiac stromal populations. In addition, *Pou5f1*, *Nanog*, and *Klf4*, but not *Tert*, also showed
333 expression in HL-1 cardiomyocytes. The expression of these stem cell-associated genes
334 (*Pou5f1*, *Klf4*, *Nanog*) has been observed in mouse cardiac stromal populations and rat
335 CDCs[56]. A sporadic expression of these markers has also been noted in primary neonatal
336 cardiomyocytes[9]. Other studies have also reported the expression of *Pou5f1*[57], *Klf4*[58],
337 *Nanog*[59,60] in adult differentiated cells. Furthermore, *Tert* is activated in human and mouse
338 primary fibroblasts to protect against malignant transformation[61]. As stem cell-associated
339 genes have been implicated in tumorigenesis and proliferation[62,63], it is not surprising to
340 observe their expression in the HL-1 cell line or the stromal populations.

341 ***Tcf21* versus *Tbx5* polarity may represent functional heterogeneity in fibroblast**
342 **populations and reveal a macrophage phenotype in a CT subpopulation.**
343 Noseda *et al*.[9] revealed an enrichment of *Tcf21* and *Pdgfra*, the cardiogenic genes *Gata4,*
344 *Mef2a/c, Tbx5/20 and Hand2*, and a lack of *Cdh5* and *Kdr* in the SCA1$^+$ SP$^+$ population in
345 comparison to total SCA1$^+$ and SCA1$^+$ SP$^-$ populations. In our study, a lack of *Cdh5* expression
346 was observed in all cardiac stromal populations. Both CTs and CDCs showed high expression
347 of the cardiogenic transcription factors *Gata4*, *Tbx20*, *Hand2*, and *Mef2a* with CTs expressing
348 *Mef2c* and CDCs expressing *Tbx5*. Interestingly, among these transcription factors, *Tbx5*
349 showed the lowest expression in the SCA1$^+$ SP$^+$ population. Moreover, these results are
350 consistent with the observations of Furtado *et al*. showing an enrichment of cardiogenic genes
351 in cardiac fibroblasts[17]. In contrast, CFs had less uniform expression of *Gata4*, *Tbx20*, and
352 *Hand2*. The PCA analysis showed an interesting polarisation between *Tcf21* and *Tbx5*, which
353 was also reflected on the correlation plot showing a strong negative correlation between the
354 two genes. Indeed, the separation in clustering of CTs and CFs can be attributed to the
355 expression of these two genes. Although it is unclear what this polarisation means, it is an
356 interesting observation that warrants further investigations in future studies as it may reflect
357 potential functional heterogeneity.

358 In addition to the enrichment of *Tcf21* in CTs as opposed to other stromal populations, the
359 macrophage-associated gene *Mrc1* was detected in a subset of CTs. This was also reflected
360 by the positive correlation between *Mrc1* and *Tcf21* versus the negative correlation between
361 *Mrc1* and *Tbx5*. *Mrc1* has been reported to show higher expression in macrophages, relative
362 to other cardiac cell types[19]. *Csf1r*, enriched in M2-polarised macrophages[64], was expressed
363 in all stromal populations, albeit at significantly higher levels in CTs. This suggests the
364 possibility of a macrophage-like subpopulation in CT populations, and potentially in CDC and
365 CF populations as well. *Csf1r* expression has also been used as an indicator of embryonic
366 myeloid lineage commitment[65]. However, cells expressing *Mrc1* or *Csf1r* showed co-
367 expression of fibroblast markers and did not show clear separation in clustering. Cells
368 expressing *Mrc1* or *Csf1r* may therefore represent the transdifferentiation of macrophages in
369 the stromal isolations into fibroblasts or *vice versa*. Indeed, the transdifferentiation of
370 macrophages to fibroblast cells has been described *in vivo*[66]. Moreover, hybrid mesenchymal
371 phenotypes have been previously described where fibroblast-associated genes are expressed
372 in minor subpopulations of macrophage or endothelial cells[19]. However, due to the lack of
373 *Cd45* expression in CTs, it is more likely that macrophage-associated genes were upregulated

374 in a subset of fibroblasts rather than *vice versa*. This phenomenon has been previously
375 reported in *in vitro* fibroblast cultures[67].

376 Our results suggest that (1) CTs were similar to CDCs and differed from CFs in their
377 expression profile, enrichment of cardiogenic factors and robustness; (2) CTs, CDCs, and CFs
378 resembled "fibroblasts 1", which are the predominant fibroblast subtype in the adult murine
379 heart; (3) CDCs clustered between CTs and CFs which separated based on their expression
380 of *Tcf21* and *Tbx5*, respectively; (4) CTs were enriched for the macrophage-associated genes
381 *Mrc1* and *Csf1r*, which may be attributed to transdifferentiation of macrophages to or from a
382 fibroblast phenotype in a subset of CTs; (5) PCA analysis revealed a transcriptional gradient
383 suggesting that heterogeneity exists within fibroblast subtypes which may reflect functional
384 heterogeneity. Overall, our findings highlight the heterogeneity of the stromal compartment of
385 the heart and how the isolation protocol may enrich for specific cell subpopulations, which may
386 ultimately affect the therapeutic potential of the cells. Furthermore, the decreased culture time
387 required to generate CTs, as compared to that for the CDCs, suggests that a CPC population
388 for therapeutic use could be achieved more efficiently.

Methods

1. Mice

C57BL/6 mice (Harlan, Oxon, UK) were kept under in a 12-hour light-dark cycle, and controlled conditions of temperature, humidity, with free access to water and chow. All animal procedures were reviewed and approved by the University of Oxford Animal Welfare and Ethical Review Board and conforms to the Animals (Scientific Procedures) Act 1986 incorporating Directive 2010/63/EU of the European Parliament.

2. Isolation and expansion of mouse CPCs

Mice were terminally anesthetised with isoflurane and hearts were isolated and washed with Dulbecco's phosphate buffered saline (DPBS) containing 50mg of primocin (antimicrobial agent; InvivoGen). Mouse atrial appendages were dissected and minced mechanically into 1 - 2 mm^3 pieces. For CT isolation, the tissue pieces were then transferred into a digestion mix (0.1% trypsin and 0.1% Collagenase II (Calbiochem, 286U/mg) in DPBS) and incubated in a water bath at 37°C for a total of 40 minutes. Every 10 minutes the digestion mix was mechanically triturated by pipetting, left on ice for 1 minute to settle and the supernatant was collected. Fresh digestion mix was added again to the tissue pieces for a total of 4 digestions. At the final digestion step, sterile 19G needles and 1ml syringes were used to triturate the tissue. After each digestion, the supernatant was neutralised, and the cell suspension was resuspended in fresh complete explant medium (CEM; Iscove's modified Dulbecco's medium supplemented with 20% FBS, 100U/ml penicillin, 100µg/ml streptomycin and 2mM L-glutamine, ThermoFisher)[11] to be plated in a 12-well plate through a 40µm cell strainer. The wells were pre-coated with 50µl per cm^2 of fibronectin (2µg/ml in DPBS; Sigma-Aldrich) and cells were allowed to attach for 3 days without media changes. For CDC isolation[11], the tissue pieces were digested in 0.05% Trypsin-EDTA (ThermoFisher) for 4 minutes at 37°C then neutralised with CEM. Processed tissue pieces were plated on fibronectin-coated (3µg/ml in DPBS) 6-well plates containing CEM and explants were cultured for 25-30 days at 37°C in 5% CO_2 with media changes every 2-3 days. When explant-derived cells (EDCs) reached 70-80% confluency, they were harvested by washing with 0.53mM Versene (ThermoFisher) before a trypsin digestion. EDCs were resuspended in Cardiosphere Growth Medium (CGM), comprising 65% Dulbecco's modified eagle medium (DMEM/F12), 35% IMDM, 7% foetal bovine serum (FBS; ThermoFisher), 2% B27 (ThermoFisher), 25ng/ml cardiotrophin (Peprotech EC), 10ng/ml epidermal growth factor (EGF; Peprotech EC), 20ng/ml basic fibroblast growth factor (FGF; Promega) and 5 units thrombin (Sigma-Aldrich), at a concentration of $2x10^4$ cells/ml and seeded as 25µl droplets on an un-coated lid of a Petri dish. DPBS was added to the Petri dishes to keep the hanging drops humid throughout 3 days of culture allowing the spherical multicellular clusters, known as cardiospheres, to form. Cardiospheres were collected by elution and gentle pipetting with DPBS and were plated in fibronectin-coated 12-well plates with CEM allowing them to spontaneously release CDCs.

3. Cell culture

Primary CPCs were cultured in CEM and plated on fibronectin-coated flasks. HL-1 cardiomyocytes[36] were maintained in Claycomb medium (Sigma-Aldrich), supplemented with 100U/ml penicillin, 100µg/ml streptomycin and 2mM L-glutamine (ThermoFisher), 100µM norepinephrine (Sigma-Aldrich) in 30mM L-ascorbic acid (Sigma-Aldrich), and 10% FBS and plated on flaks pre-coated with 0.02% (wt/vol) gelatin (Sigma-Aldrich) containing 5µg/ml fibronectin. C57BL/6 adult mouse atrial primary cardiac fibroblasts, obtained from Cell Biologics (USA), were maintained in complete fibroblast medium (Cell Biologics – USA) supplemented with the provided supplement kit: FGF, hydrocortisone, L-glutamine, Antibiotic-Antimycotic Solution, and 10% FBS and plated on flasks pre-coated with 0.02% (wt/vol) gelatin. For serum starvation experiments, cells were switched to serum-free media for 72 hours.

4. Single-cell qRT-PCR

Single cells were sorted directly (FACSAria II) into 96-well plates containing the reaction mixture for pre-amplification, using CellsDirect One-Step qRT–PCR Kits (ThermoFisher). Pre-

442 amplification was performed in a Veriti Thermal Cycler (Applied Biosystems) for 22 cycles. As
443 negative controls, at least 3–5 non-template samples were included in each run at the pre-
444 amplification stage. Quantitative amplification was performed using Dynamic Array chips for
445 48 assays x 48 samples, the BioMark HD system (Fluidigm) and TaqMan probes (Appendix
446 D) according to manufacturer's instructions. Each sample was normalised to ΔCt using the
447 expression of *Ubc*. As described in Noseda *et al*. 2015[9], data were plotted in colour-coded
448 heatmaps of inverted ΔCt values (blue is low or absent; red is high). Samples were ordered
449 based on cell type, and the genes grouped by a hierarchical clustering algorithm based on the
450 underlying co-expression pattern. Differences between samples were investigated using PCA.
451 PCA applies multiple linear transformations (singular value decomposition) to the expression
452 profiles (standardised ΔCt values) of individual samples, and identifies a series of PCs that
453 elucidate the most distinguishing features between the samples. The linear projections (PC
454 scores) attempt to maximise the variation between the samples, whereas the coefficients of
455 those projections (PC loadings) measure the importance of genes in defining the underlying
456 variability associated with each component.

457 **Taqman probes used for single-cell qRT-PCR**

Mesp1	Mm00801883_g1	*Nkx2-5*	Mm00657783_m1
Mef2c	Mm01340842_m1	*Myh11*	Mm00443013_m1
Mef2a	Mm01318990_m1	*Cnn1*	Mm00487032_m1
Hand1	Mm00433931_m1	*αSMA (Acta2)*	Mm01546133_m1
Islet1 (Isl1)	Mm00627860_m1	*Vim*	Mm01333430_m1
Tbx20	Mm00451515_m1	*Cd44*	Mm01277163_m1
Gata4	Mm00484689_m1	*Pdgfrb*	Mm00435546_m1
Hand2	Mm00439247_m1	*Ng2*	Mm01283063_m1
Tbx5	Mm00803518_m1	*Ddr2*	Mm00445615_m1
Ly6a (Sca1)	Mm00726565_s1	*Medag*	Mm00551008_m1
Wt1	Mm00460570_m1	*Ms4a4d*	Mm00656404_m1
Klf4	Mm00516104_m1	*Col1a1*	Mm00801666_g1
Pou5f1 (Oct4)	Mm03053917_g1	*Prg4*	Mm01284582_m1
Nanog	Mm02019550_s1	*Wif1*	Mm00442355_m1
Tert	Mm0352136_m1	*Colec11*	Mm01289834_m1
Kdr	Mm00440111_m1	*Kcnj8*	Mm00434620_m1
Cdh5	Mm00486938_m1	*Mrc1*	Mm01329362_m1
Vwf	Mm00550376_m1	*Cx3cr1*	Mm00438354_m1
Pdgfra	Mm01211685_m1	*Csf1 r*	Mm01266652_m1
Tcf21	Mm00448961_m1	*Kcna1*	Mm00439977_s1
Myl2	Mm00440384_m1	*Plp1*	Mm01297210_m1
Myh6	Mm00440359_m1	*Ptprc (Cd45)*	Mm01293577_m1
Nppa	Mm01255748_g1	*Ubc*	Mm01201237_m1
Hmbs	Mm01143545_m1		

458

459 **Supplementary Table 1.** Description of the markers used in the single-cell qRT-PCR
460 characterisation.
461

Gene	*Full name of encoded protein*	*Type*	*Relevant expression pattern*	*Relevant function*	*Refere-nces*
Cd44	Cluster of differentiation 44	Transmembrane glycoprotein	Fibroblasts, macrophages, endothelial cells	Cellular adhesion; angiogenesis; release of cytokines; regulates inflammation and fibrosis	68-71
Cdh5	Cadherin 5 or VE-cadherin	Member of the cadherin family of calcium-dependent glycoproteins	Endothelial cells	Calcium-dependent cell adhesion; cell proliferation and migration	68,72
Col1a1	Collagen, type I, alpha 1	Member of group I collagen	Fibroblasts, smooth muscle cells	Collagen type I synthesis	68,73
Colec11	Collectin subfamily member 11	Member of the collectin family of C-type lectins	Pericytes, endothelial cells	Collectins are initiators of the lectin complement pathway, which is integral to the innate immune response; embryogenesis	19,68,74,75
Csf1r	Colony-stimulating factor 1 receptor	Receptor tyrosine kinase	Macrophages (used as an M2 marker)	Growth and differentiation of macrophages; maintenance of the intestinal stem cell niche	64,76
Cx3cr1	CX3C chemokine receptor 1	Member of the 7-transmembrane G protein-coupled receptor family	Macrophages	Macrophage survival and function	68,77,78
Ddr2	Discoidin domain receptor tyrosine kinase 2 or CD167b	Receptor tyrosine kinase	Fibroblasts, smooth muscle cells, pericytes	Activated by collagen binding; cell proliferation; adhesion and migration; ECM degradation	68,79,80
Gata4	GATA binding factor 4	Transcription factor of the zinc-finger GATA family	Cardiomyocytes, cardiac fibroblasts	Cardiogenesis	17,18,81-83
Hand1	Heart- and neural crest derivatives-expressed protein 1	Transcription factor of the basic helix-loop-helix family	FHF, reported to be undetectable in adult mouse hearts	Cardiogenesis; epicardial development and coronary vessel formation	84-87
Hand2	Heart- and neural crest derivatives-expressed protein 2	Transcription factor of the basic helix-loop-helix family	SHF, cardiomyocytes, endothelial cells, fibroblasts	Cardiogenesis; epicardial development and coronary vessel formation	9,18,84,85,87
Isl1	Insulin gene enhancer protein 1	Transcription factor of the LIM/homeodomain family	CPCs, cardiac neural crest, endothelial cells	Cardiogenesis	28,40-42,88
Kcna1	Potassium voltage-gated channel subfamily A member 1	Member of the 6-TM family	Schwann cells	Regulator of membrane excitability	19,68,89
Kcnj8	Potassium inwardly-rectifying channel, subfamily J, member 8	The inward-rectifier potassium channel family (also known as 2-TM channels)	Pericytes	Regulator of vascular tone and cardiac adaptive response to systemic metabolic stressors	19,68,90-92
Kdr	Kinase insert domain receptor or foetal liver kinase 1 (FLK1); VEGFR2; CD309	Receptor tyrosine kinase	Endothelial cells, Kdr^+ developmental cardiovascular progenitor	Transduction of VEGF-A effects	43,44,68,93
Klf4	Krüppel like factor 4	Member of the Krüppel-like family of transcription factors	Stem cells, endothelial cells, fibroblasts	Pluripotency; angiogenesis; embryonic vasculogenesis; myofibroblast differentiation	58,68,94-96
Medag	Mesenteric oestrogen-dependent	Member of the sex-steroid regulated mesenteric	Cardiac fibroblasts “1”	Adipogenesis; glucose uptake; interacts with the fatty acid	19,97,98

	adipogenesis protein	oestrogen- dependent adipogenesis proteins		transporter CD36 that is involved in the uptake of apoptotic material	
Mef2a	Myocyte-specific enhancer factor 2A	Transcription factor of the MEF2 family	Cardiomyocytes, cardiac fibroblasts, endothelial cells, smooth muscle cells, macrophages and pericytes	Cardiogenesis; vasculogenesis	9,68,99,100
Mef2c	Myocyte-specific enhancer factor 2C or MADS box transcription enhancer factor 2	Transcription factor of the MEF2 family	Cardiomyocytes, cardiac fibroblasts, endothelial cells, smooth muscle cells, macrophages and pericytes	Cardiogenesis; vasculogenesis	9,17,18,68,83,101,102
Mesp1	Mesoderm Posterior Transcription Factor 1	Transcription factor of the basic helix-loop-helix family	Mesoderm	Development of cardiac mesoderm	103
Mrc1	Mannose receptor C-type 1 or CD206	Transmembrane glycoprotein	Macrophages (used as an M2 marker)	Mediates the endocytic functions by macrophages and the DNA replication checkpoint	19,68,104-106
Ms4a4d	Membrane-spanning 4-domains subfamily A member 4D	Member of the membrane-spanning 4A (MS4A) family	Cardiac fibroblasts “1”, reported to be expressed in M2 macrophages	May have a role as an adaptor protein to facilitate intracellular protein–protein interactions. Its functionality is still not fully understood.	19,107,108
Myh6	Myosin heavy chain 6 or αMHC	Hexameric ATPase cellular motor protein	Predominantly atrial cardiomyocytes	Cardiogenesis; force generation and muscle contraction	109
Myl2	Myosin light chain 2	Hexameric ATPase cellular motor protein	Predominantly ventricular cardiomyocytes	Cardiogenesis; force generation and muscle contraction	109
Nanog	Nanog Homeobox	Transcription factor of the Nanog homeobox family	Stem cells	Pluripotency; tumourigenicity	59,60,110
Ng2	Neuron-glial antigen 2 or chondroitin sulphate proteoglycan 4	Transmembrane proteoglycan	Pericytes, smooth muscle cells	Co-receptor in conjunction with PDGFRα; angiogenesis; cell survival and migration	68,111-113
Nkx2-5	NK2 homeobox 5	Transcription factor of the NK-2 homeobox family	Cardiomyocytes	Cardiogenesis	68,114
Nppa	Natriuretic Peptide A	The natriuretic peptide family	Predominantly atrial cardiomyocytes	Cardiac hormone involved in regulating blood volume and pressure and cardiovascular homeostasis	115
Pou5f1	Octamer-binding transcription factor 4 (Oct4) or POU class 5 homeobox 1	Transcription factor of the homeodomain POU (Pit-Oct-Unc) family.	Stem cells	Pluripotency; tumourigenicity	116,117
Pdgfra	Platelet-derived growth factor receptor α	Receptor tyrosine kinase	Fibroblasts, defines the $SCA1^{+}SP^{+}$ population (CPCs)	Development of mesenchymal cell types; cardiogenesis	9,68,118-120
Pdgfrb	Platelet-derived growth factor receptor β	Receptor tyrosine kinase	Pericytes, fibroblasts, endothelial cells, smooth muscle cells	Development of mesenchymal cell types; regulation of autophagic processes; cell proliferation and survival; adult mammalian cardiomyocyte proliferation; cardiogenesis	68,120-126
Plp1	Proteolipid protein 1	Myelin proteolipid protein	Schwann cells, endothelial cells, smooth muscle cells,	Myelination	127

			pericytes and macrophages		
Prg4	Proteoglycan 4	Mucinous glycoprotein	Cardiac fibroblasts “2”	Ligand for CD44 receptor, ECM constituent conferring compression resistance	19,128,129
Ptprc (Cd45)	Protein tyrosine phosphatase, receptor type, C	Transmembrane glycoprotein	Haematopoietic cells (except erythrocytes and plasma cells)	Haematopoietic cell activation and differentiation and immune Function	130-132
Ly6a	Stem cell antigen 1 (SCA1) or lymphocyte antigen 6 complex	Glycosyl phosphatidylinositol-anchored cell surface protein of the LY6 gene family	HSCs, fibroblasts, endothelial cells, CPCs	Tumourigenicity; cell migration; HSC self-renewal and fate determination	9,68,133-136
Tbx20	T-box 20	Transcription factor of the T-box family	Cardiomyocytes, cardiac pericytes and fibroblasts	Cardiogenesis	9,68
Tbx5	T-box 5	Transcription factor of the T-box family	Cardiomyocytes, cardiac fibroblasts	Cardiogenesis	17,18,83
Tcf21	Transcription factor 21	Transcription factor of the basic helix-loop-helix family	Epicardium, Cardiac fibroblasts “1”	Initiation of epicardial EMT for fibroblast development; proepicardial cell specification	19,49,137
Tert	Telomerase reverse transcriptase	Member of the reverse transcriptase family	Stem and progenitor cells	Cellular immortalisation tumourigenicity; cell proliferation	138,139
Vim	Vimentin or fibroblast intermediate filament	Type III intermediate filament protein	Fibroblasts, endothelial cell, smooth muscle cells, Schwann cells	Maintenance of cellular integrity; EMT; protective role against nuclear rupture and DNA damage during cell migration.	35,68
Vwf	von Willebrand factor	Adhesive plasma glycoprotein	Endothelial cells	Platelet adhesion and aggregation	140
Wif1	WNT inhibitory factor 1	Lipid-binding protein	Cardiac fibroblasts “2”	Mesoderm segmentation; cardiogenesis	19,141
Wt1	Wilms tumour 1	Transcription factor with proline / glutamine- rich DNA- binding domain	Epicardium, fibroblasts, endothelial cells, macrophages	Epicardial EMT; vasculogenesis	17,54,55,142,143
Acta2	Alpha smooth muscle actin (αSMA) or Actin alpha 2	Member of the globular Actin proteins family	Smooth muscle cells, myofibroblasts, pericytes	Cell motility and contractility	34,144

462

Author contributions

Conceptualisation: RA, NS, CC. Investigation: RA, PCG, SS, MN. Funding acquisition: RA. Writing: RA, CC.

Declaration of interests

None

Acknowledgements

This work was supported by the King Faisal Specialist Hospital & Research Centre (PhD scholarship to RA).

473 **References**

474 1 Ali, S. R. *et al.* Existing cardiomyocytes generate cardiomyocytes at a low rate after
475 birth in mice. *Proc Natl Acad Sci U S A* **111**, 8850-8855 (2014).
476 https://doi.org/10.1073/pnas.1408233111

477 2 Kimura, W. *et al.* Corrigendum: Hypoxia fate mapping identifies cycling
478 cardiomyocytes in the adult heart. *Nature* **532**, 268 (2016).
479 https://doi.org/10.1038/nature16177

480 3 Senyo, S. E. *et al.* Mammalian heart renewal by pre-existing cardiomyocytes. *Nature*
481 **493**, 433-436 (2013). https://doi.org/10.1038/nature11682

482 4 Alonaizan, R. & Carr, C. Cardiac regeneration following myocardial infarction: the need
483 for regeneration and a review of cardiac stromal cell populations used for
484 transplantation. *Biochem Soc Trans* **50**, 269-281 (2022).
485 https://doi.org/10.1042/BST20210231

486 5 Eschenhagen, T. *et al.* Cardiomyocyte Regeneration: A Consensus Statement.
487 *Circulation* **136**, 680-686 (2017).
488 https://doi.org/10.1161/CIRCULATIONAHA.117.029343

489 6 Li, Y. *et al.* Genetic Tracing Identifies Early Segregation of the Cardiomyocyte and
490 Nonmyocyte Lineages. *Circ Res* **125**, 343-355 (2019).
491 https://doi.org/10.1161/CIRCRESAHA.119.315280

492 7 Carr, C. A. *et al.* Cardiosphere-derived cells improve function in the infarcted rat heart
493 for at least 16 weeks--an MRI study. *PLoS One* **6**, e25669 (2011).
494 https://doi.org/10.1371/journal.pone.0025669

495 8 Lee, S. T. *et al.* Intramyocardial injection of autologous cardiospheres or cardiosphere-
496 derived cells preserves function and minimizes adverse ventricular remodeling in pigs
497 with heart failure post-myocardial infarction. *J Am Coll Cardiol* **57**, 455-465 (2011).
498 https://doi.org/10.1016/j.jacc.2010.07.049

499 9 Noseda, M. *et al.* PDGFRalpha demarcates the cardiogenic clonogenic Sca1+
500 stem/progenitor cell in adult murine myocardium. *Nat Commun* **6**, 6930 (2015).
501 https://doi.org/10.1038/ncomms7930

502 10 Smart, N. *et al.* De novo cardiomyocytes from within the activated adult heart after
503 injury. *Nature* **474**, 640-644 (2011). https://doi.org/10.1038/nature10188

504 11 Smith, R. R. *et al.* Regenerative potential of cardiosphere-derived cells expanded from
505 percutaneous endomyocardial biopsy specimens. *Circulation* **115**, 896-908 (2007).
506 https://doi.org/10.1161/CIRCULATIONAHA.106.655209

507 12 Caplan, A. I. All MSCs are pericytes? *Cell Stem Cell* **3**, 229-230 (2008).
508 https://doi.org/10.1016/j.stem.2008.08.008

509 13 Denu, R. A. *et al.* Fibroblasts and Mesenchymal Stromal/Stem Cells Are Phenotypically
510 Indistinguishable. *Acta Haematol* **136**, 85-97 (2016).
511 https://doi.org/10.1159/000445096

512 14 Hematti, P. Mesenchymal stromal cells and fibroblasts: a case of mistaken identity?
513 *Cytotherapy* **14**, 516-521 (2012). https://doi.org/10.3109/14653249.2012.677822

514 15 Murray, I. R. & Peault, B. Q&A: Mesenchymal stem cells - where do they come from
515 and is it important? *BMC Biol* **13**, 99 (2015). https://doi.org/10.1186/s12915-015-
516 0212-7

517 16 Soundararajan, M. & Kannan, S. Fibroblasts and mesenchymal stem cells: Two sides of
518 the same coin? *J Cell Physiol* **233**, 9099-9109 (2018).
519 https://doi.org/10.1002/jcp.26860

520 17 Furtado, M. B. *et al.* Cardiogenic genes expressed in cardiac fibroblasts contribute to
521 heart development and repair. *Circ Res* **114**, 1422-1434 (2014).
522 https://doi.org/10.1161/CIRCRESAHA.114.302530

523 18 Furtado, M. B. *et al.* Microarray profiling to analyse adult cardiac fibroblast identity.
524 *Genom Data* **2**, 345-350 (2014). https://doi.org/10.1016/j.gdata.2014.10.006

525 19 Skelly, D. A. *et al.* Single-Cell Transcriptional Profiling Reveals Cellular Diversity and
526 Intercommunication in the Mouse Heart. *Cell Rep* **22**, 600-610 (2018).
527 https://doi.org/10.1016/j.celrep.2017.12.072

528 20 Vicinanza, C. *et al.* Adult cardiac stem cells are multipotent and robustly myogenic: c-
529 kit expression is necessary but not sufficient for their identification. *Cell Death Differ*
530 **24**, 2101-2116 (2017). https://doi.org/10.1038/cdd.2017.130

531 21 Chan, H. H. *et al.* Human cardiosphere-derived cells from patients with chronic
532 ischaemic heart disease can be routinely expanded from atrial but not epicardial
533 ventricular biopsies. *J Cardiovasc Transl Res* **5**, 678-687 (2012).
534 https://doi.org/10.1007/s12265-012-9389-0

535 22 Gharaibeh, B. *et al.* Isolation of a slowly adhering cell fraction containing stem cells
536 from murine skeletal muscle by the preplate technique. *Nat Protoc* **3**, 1501-1509
537 (2008). https://doi.org/10.1038/nprot.2008.142

538 23 Okada, M. *et al.* Human skeletal muscle cells with a slow adhesion rate after isolation
539 and an enhanced stress resistance improve function of ischemic hearts. *Mol Ther* **20**,
540 138-145 (2012). https://doi.org/10.1038/mt.2011.229

541 24 Malandraki-Miller, S. *et al.* Metabolic flux analyses to assess the differentiation of
542 adult cardiac progenitors after fatty acid supplementation. *Stem Cell Res* **38**, 101458
543 (2019). https://doi.org/10.1016/j.scr.2019.101458

544 25 Goumans, M. J. *et al.* TGF-beta1 induces efficient differentiation of human
545 cardiomyocyte progenitor cells into functional cardiomyocytes in vitro. *Stem Cell Res*
546 **1**, 138-149 (2007). https://doi.org/10.1016/j.scr.2008.02.003

547 26 Smits, A. M. *et al.* Human cardiomyocyte progenitor cells differentiate into functional
548 mature cardiomyocytes: an in vitro model for studying human cardiac physiology and
549 pathophysiology. *Nat Protoc* **4**, 232-243 (2009).
550 https://doi.org/10.1038/nprot.2008.229

551 27 Lopaschuk, G. D. & Jaswal, J. S. Energy metabolic phenotype of the cardiomyocyte
552 during development, differentiation, and postnatal maturation. *J Cardiovasc*
553 *Pharmacol* **56**, 130-140 (2010). https://doi.org/10.1097/FJC.0b013e3181e74a14

554 28 Laugwitz, K. L. *et al.* Postnatal isl1+ cardioblasts enter fully differentiated
555 cardiomyocyte lineages. *Nature* **433**, 647-653 (2005).
556 https://doi.org/10.1038/nature03215

557 29 Ye, J. *et al.* Sca-1+ cardiosphere-derived cells are enriched for Isl1-expressing cardiac
558 precursors and improve cardiac function after myocardial injury. *PLoS One* **7**, e30329
559 (2012). https://doi.org/10.1371/journal.pone.0030329

560 30 Lu, C. *et al.* Serum starvation induces H2AX phosphorylation to regulate apoptosis via
561 p38 MAPK pathway. *FEBS Lett* **582**, 2703-2708 (2008).
562 https://doi.org/10.1016/j.febslet.2008.06.051

563 31 Huang, Y. C. *et al.* Isolation of mesenchymal stem cells from human placental decidua
564 basalis and resistance to hypoxia and serum deprivation. *Stem Cell Rev Rep* **5**, 247-255
565 (2009). https://doi.org/10.1007/s12015-009-9069-x

566 32 Peng, L. *et al.* Comparative analysis of mesenchymal stem cells from bone marrow,
567 cartilage, and adipose tissue. *Stem Cells Dev* **17**, 761-773 (2008).
568 https://doi.org/10.1089/scd.2007.0217

569 33 Liberio, M. S., Sadowski, M. C., Soekmadji, C., Davis, R. A. & Nelson, C. C. Differential
570 effects of tissue culture coating substrates on prostate cancer cell adherence,
571 morphology and behavior. *PLoS One* **9**, e112122 (2014).
572 https://doi.org/10.1371/journal.pone.0112122

573 34 Rockey, D. C., Weymouth, N. & Shi, Z. Smooth muscle alpha actin (Acta2) and
574 myofibroblast function during hepatic wound healing. *PLoS One* **8**, e77166 (2013).
575 https://doi.org/10.1371/journal.pone.0077166

576 35 Patteson, A. E. *et al.* Vimentin protects cells against nuclear rupture and DNA damage
577 during migration. *J Cell Biol* **218**, 4079-4092 (2019).
578 https://doi.org/10.1083/jcb.201902046

579 36 Claycomb, W. C. *et al.* HL-1 cells: a cardiac muscle cell line that contracts and retains
580 phenotypic characteristics of the adult cardiomyocyte. *Proc Natl Acad Sci U S A* **95**,
581 2979-2984 (1998). https://doi.org/10.1073/pnas.95.6.2979

582 37 Kuznetsov, A. V., Javadov, S., Sickinger, S., Frotschnig, S. & Grimm, M. H9c2 and HL-1
583 cells demonstrate distinct features of energy metabolism, mitochondrial function and
584 sensitivity to hypoxia-reoxygenation. *Biochim Biophys Acta* **1853**, 276-284 (2015).
585 https://doi.org/10.1016/j.bbamcr.2014.11.015

586 38 Geraghty, R. J. *et al.* Guidelines for the use of cell lines in biomedical research. *Br J*
587 *Cancer* **111**, 1021-1046 (2014). https://doi.org/10.1038/bjc.2014.166

588 39 Volz, K. S. *et al.* Pericytes are progenitors for coronary artery smooth muscle. *Elife* **4**
589 (2015). https://doi.org/10.7554/eLife.10036

590 40 Moretti, A. *et al.* Multipotent embryonic isl1+ progenitor cells lead to cardiac, smooth
591 muscle, and endothelial cell diversification. *Cell* **127**, 1151-1165 (2006).
592 https://doi.org/10.1016/j.cell.2006.10.029

593 41 Lam, J. T., Moretti, A. & Laugwitz, K. L. Multipotent progenitor cells in regenerative
594 cardiovascular medicine. *Pediatr Cardiol* **30**, 690-698 (2009).
595 https://doi.org/10.1007/s00246-009-9450-1

596 42 Weinberger, F. *et al.* Localization of Islet-1-positive cells in the healthy and infarcted
597 adult murine heart. *Circ Res* **110**, 1303-1310 (2012).
598 https://doi.org/10.1161/CIRCRESAHA.111.259630

599 43 Kattman, S. J., Huber, T. L. & Keller, G. M. Multipotent flk-1+ cardiovascular progenitor
600 cells give rise to the cardiomyocyte, endothelial, and vascular smooth muscle lineages.
601 *Dev Cell* **11**, 723-732 (2006). https://doi.org/10.1016/j.devcel.2006.10.002

602 44 Motoike, T., Markham, D. W., Rossant, J. & Sato, T. N. Evidence for novel fate of Flk1+
603 progenitor: contribution to muscle lineage. *Genesis* **35**, 153-159 (2003).
604 https://doi.org/10.1002/gene.10175

605 45 Mekala, S. R. *et al.* Generation of Cardiomyocytes From Vascular Adventitia-Resident
606 Stem Cells. *Circ Res* **123**, 686-699 (2018).
607 https://doi.org/10.1161/CIRCRESAHA.117.312526

608 46 Zampetaki, A., Kirton, J. P. & Xu, Q. Vascular repair by endothelial progenitor cells.
609 *Cardiovasc Res* **78**, 413-421 (2008). https://doi.org/10.1093/cvr/cvn081

610 47 Gao, L. *et al.* Single-cell transcriptomics of cardiac progenitors reveals functional
611 subpopulations and their cooperative crosstalk in cardiac repair. *Protein Cell* **12**, 152-
612 157 (2021). https://doi.org/10.1007/s13238-020-00788-6

613 48 Masters, M. & Riley, P. R. The epicardium signals the way towards heart regeneration.
614 *Stem Cell Res* **13**, 683-692 (2014). https://doi.org/10.1016/j.scr.2014.04.007

615 49 Acharya, A. *et al.* The bHLH transcription factor Tcf21 is required for lineage-specific
616 EMT of cardiac fibroblast progenitors. *Development* **139**, 2139-2149 (2012).
617 https://doi.org/10.1242/dev.079970

618 50 Braitsch, C. M., Kanisicak, O., van Berlo, J. H., Molkentin, J. D. & Yutzey, K. E.
619 Differential expression of embryonic epicardial progenitor markers and localization of
620 cardiac fibrosis in adult ischemic injury and hypertensive heart disease. *J Mol Cell*
621 *Cardiol* **65**, 108-119 (2013). https://doi.org/10.1016/j.yjmcc.2013.10.005

622 51 Kanisicak, O. *et al.* Genetic lineage tracing defines myofibroblast origin and function in
623 the injured heart. *Nat Commun* **7**, 12260 (2016).
624 https://doi.org/10.1038/ncomms12260

625 52 Armstrong, J. F., Pritchard-Jones, K., Bickmore, W. A., Hastie, N. D. & Bard, J. B. The
626 expression of the Wilms' tumour gene, WT1, in the developing mammalian embryo.
627 *Mech Dev* **40**, 85-97 (1993). https://doi.org/10.1016/0925-4773(93)90090-k

628 53 Carmona, R., Gonzalez-Iriarte, M., Perez-Pomares, J. M. & Munoz-Chapuli, R.
629 Localization of the Wilm's tumour protein WT1 in avian embryos. *Cell Tissue Res* **303**,
630 173-186 (2001). https://doi.org/10.1007/s004410000307

631 54 Duim, S. N., Kurakula, K., Goumans, M. J. & Kruithof, B. P. Cardiac endothelial cells
632 express Wilms' tumor-1: Wt1 expression in the developing, adult and infarcted heart.
633 *J Mol Cell Cardiol* **81**, 127-135 (2015). https://doi.org/10.1016/j.yjmcc.2015.02.007

634 55 Sanz-Morejon, A. *et al.* Wilms Tumor 1b Expression Defines a Pro-regenerative
635 Macrophage Subtype and Is Required for Organ Regeneration in the Zebrafish. *Cell*
636 *Rep* **28**, 1296-1306 e1296 (2019). https://doi.org/10.1016/j.celrep.2019.06.091

637 56 Tan, S. C. *et al.* Preconditioning of Cardiosphere-Derived Cells With Hypoxia or Prolyl-
638 4-Hydroxylase Inhibitors Increases Stemness and Decreases Reliance on Oxidative
639 Metabolism. *Cell Transplant* **25**, 35-53 (2016).
640 https://doi.org/10.3727/096368915X687697

641 57 Zangrossi, S. *et al.* Oct-4 expression in adult human differentiated cells challenges its
642 role as a pure stem cell marker. *Stem Cells* **25**, 1675-1680 (2007).
643 https://doi.org/10.1634/stemcells.2006-0611

644 58 Ghaleb, A. M. & Yang, V. W. Kruppel-like factor 4 (KLF4): What we currently know.
645 *Gene* **611**, 27-37 (2017). https://doi.org/10.1016/j.gene.2017.02.025

646 59 Ambady, S. *et al.* Expression of NANOG and NANOGP8 in a variety of undifferentiated
647 and differentiated human cells. *Int J Dev Biol* **54**, 1743-1754 (2010).
648 https://doi.org/10.1387/ijdb.103192sa

649 60 Piazzolla, D. *et al.* Lineage-restricted function of the pluripotency factor NANOG in
650 stratified epithelia. *Nat Commun* **5**, 4226 (2014).
651 https://doi.org/10.1038/ncomms5226

652 61 Sun, L. *et al.* Transient induction of telomerase expression mediates senescence and
653 reduces tumorigenesis in primary fibroblasts. *Proc Natl Acad Sci U S A* **116**, 18983-
654 18993 (2019). https://doi.org/10.1073/pnas.1907199116

655 62 Wang, G., Zhou, H., Gu, Z., Gao, Q. & Shen, G. Oct4 promotes cancer cell proliferation
656 and migration and leads to poor prognosis associated with the survivin/STAT3
657 pathway in hepatocellular carcinoma. *Oncol Rep* **40**, 979-987 (2018).
658 https://doi.org/10.3892/or.2018.6491

659 63 White, M. G. *et al.* Pluripotency-associated stem cell marker expression in proliferative
660 cell cultures derived from adult human pancreas. *J Endocrinol* **211**, 169-176 (2011).
661 https://doi.org/10.1530/JOE-11-0123

662 64 Cannarile, M. A. *et al.* Colony-stimulating factor 1 receptor (CSF1R) inhibitors in cancer
663 therapy. *J Immunother Cancer* **5**, 53 (2017). https://doi.org/10.1186/s40425-017-
664 0257-y

665 65 Plein, A., Fantin, A., Denti, L., Pollard, J. W. & Ruhrberg, C. Erythro-myeloid progenitors
666 contribute endothelial cells to blood vessels. *Nature* **562**, 223-228 (2018).
667 https://doi.org/10.1038/s41586-018-0552-x

668 66 Sinha, M. *et al.* Direct conversion of injury-site myeloid cells to fibroblast-like cells of
669 granulation tissue. *Nat Commun* **9**, 936 (2018). https://doi.org/10.1038/s41467-018-
670 03208-w

671 67 Feng, R. *et al.* PU.1 and C/EBPalpha/beta convert fibroblasts into macrophage-like
672 cells. *Proc Natl Acad Sci U S A* **105**, 6057-6062 (2008).
673 https://doi.org/10.1073/pnas.0711961105

674 68 Franzen, O., Gan, L. M. & Bjorkegren, J. L. M. PanglaoDB: a web server for exploration
675 of mouse and human single-cell RNA sequencing data. *Database (Oxford)* **2019** (2019).
676 https://doi.org/10.1093/database/baz046

677 69 Huebener, P. *et al.* CD44 is critically involved in infarct healing by regulating the
678 inflammatory and fibrotic response. *J Immunol* **180**, 2625-2633 (2008).
679 https://doi.org/10.4049/jimmunol.180.4.2625

680 70 Sneath, R. J. & Mangham, D. C. The normal structure and function of CD44 and its role
681 in neoplasia. *Mol Pathol* **51**, 191-200 (1998). https://doi.org/10.1136/mp.51.4.191

682 71 Suleiman, M., Abdulrahman, N., Yalcin, H. & Mraiche, F. The role of CD44, hyaluronan
683 and NHE1 in cardiac remodeling. *Life Sci* **209**, 197-201 (2018).
684 https://doi.org/10.1016/j.lfs.2018.08.009

685 72 Harris, E. S. & Nelson, W. J. VE-cadherin: at the front, center, and sides of endothelial
686 cell organization and function. *Curr Opin Cell Biol* **22**, 651-658 (2010).
687 https://doi.org/10.1016/j.ceb.2010.07.006

688 73 Pan, X., Chen, Z., Huang, R., Yao, Y. & Ma, G. Transforming growth factor beta1 induces
689 the expression of collagen type I by DNA methylation in cardiac fibroblasts. *PLoS One*
690 **8**, e60335 (2013). https://doi.org/10.1371/journal.pone.0060335

691 74 Sandri, T. L. *et al.* Human collectin-11 (COLEC11) and its synergic genetic interaction
692 with MASP2 are associated with the pathophysiology of Chagas Disease. *PLoS Negl*
693 *Trop Dis* **13**, e0007324 (2019). https://doi.org/10.1371/journal.pntd.0007324

694 75 Selman, L. & Hansen, S. Structure and function of collectin liver 1 (CL-L1) and collectin
695 11 (CL-11, CL-K1). *Immunobiology* **217**, 851-863 (2012).
696 https://doi.org/10.1016/j.imbio.2011.12.008

697 76 Sehgal, A. *et al.* The role of CSF1R-dependent macrophages in control of the intestinal
698 stem-cell niche. *Nat Commun* **9**, 1272 (2018). https://doi.org/10.1038/s41467-018-
699 03638-6

700 77 Lee, M., Lee, Y., Song, J., Lee, J. & Chang, S. Y. Tissue-specific Role of CX(3)CR1
701 Expressing Immune Cells and Their Relationships with Human Disease. *Immune Netw*
702 **18**, e5 (2018). https://doi.org/10.4110/in.2018.18.e5

703 78 Zheng, J. *et al.* Chemokine receptor CX3CR1 contributes to macrophage survival in
704 tumor metastasis. *Mol Cancer* **12**, 141 (2013). https://doi.org/10.1186/1476-4598-12-
705 141

706 79 Leitinger, B. Discoidin domain receptor functions in physiological and pathological
707 conditions. *Int Rev Cell Mol Biol* **310**, 39-87 (2014). https://doi.org/10.1016/B978-0-
708 12-800180-6.00002-5

709 80 Valiathan, R. R., Marco, M., Leitinger, B., Kleer, C. G. & Fridman, R. Discoidin domain
710 receptor tyrosine kinases: new players in cancer progression. *Cancer Metastasis Rev*
711 **31**, 295-321 (2012). https://doi.org/10.1007/s10555-012-9346-z

712 81 Molkentin, J. D., Lin, Q., Duncan, S. A. & Olson, E. N. Requirement of the transcription
713 factor GATA4 for heart tube formation and ventral morphogenesis. *Genes Dev* **11**,
714 1061-1072 (1997). https://doi.org/10.1101/gad.11.8.1061

715 82 Watt, A. J., Battle, M. A., Li, J. & Duncan, S. A. GATA4 is essential for formation of the
716 proepicardium and regulates cardiogenesis. *Proc Natl Acad Sci U S A* **101**, 12573-12578
717 (2004). https://doi.org/10.1073/pnas.0400752101

718 83 Xin, M., Olson, E. N. & Bassel-Duby, R. Mending broken hearts: cardiac development
719 as a basis for adult heart regeneration and repair. *Nat Rev Mol Cell Biol* **14**, 529-541
720 (2013). https://doi.org/10.1038/nrm3619

721 84 Barnes, R. M. *et al.* Hand2 loss-of-function in Hand1-expressing cells reveals distinct
722 roles in epicardial and coronary vessel development. *Circ Res* **108**, 940-949 (2011).
723 https://doi.org/10.1161/CIRCRESAHA.110.233171

724 85 McFadden, D. G. *et al.* The Hand1 and Hand2 transcription factors regulate expansion
725 of the embryonic cardiac ventricles in a gene dosage-dependent manner.
726 *Development* **132**, 189-201 (2005). https://doi.org/10.1242/dev.01562

727 86 Thattaliyath, B. D., Livi, C. B., Steinhelper, M. E., Toney, G. M. & Firulli, A. B. HAND1
728 and HAND2 are expressed in the adult-rodent heart and are modulated during cardiac
729 hypertrophy. *Biochem Biophys Res Commun* **297**, 870-875 (2002).
730 https://doi.org/10.1016/s0006-291x(02)02297-0

731 87 Tsuchihashi, T. *et al.* Hand2 function in second heart field progenitors is essential for
732 cardiogenesis. *Dev Biol* **351**, 62-69 (2011).
733 https://doi.org/10.1016/j.ydbio.2010.12.023

734 88 Cai, C. L. *et al.* Isl1 identifies a cardiac progenitor population that proliferates prior to
735 differentiation and contributes a majority of cells to the heart. *Dev Cell* **5**, 877-889
736 (2003). https://doi.org/10.1016/s1534-5807(03)00363-0

737 89 Glasscock, E. Kv1.1 channel subunits in the control of neurocardiac function. *Channels*
738 *(Austin)* **13**, 299-307 (2019). https://doi.org/10.1080/19336950.2019.1635864

739 90 Miki, T. *et al.* Mouse model of Prinzmetal angina by disruption of the inward rectifier
740 Kir6.1. *Nat Med* **8**, 466-472 (2002). https://doi.org/10.1038/nm0502-466

741 91 Tester, D. J. *et al.* Loss-of-function mutations in the KCNJ8-encoded Kir6.1 K(ATP)
742 channel and sudden infant death syndrome. *Circ Cardiovasc Genet* **4**, 510-515 (2011).
743 https://doi.org/10.1161/CIRCGENETICS.111.960195

744 92 Zingman, L. V., Alekseev, A. E., Hodgson-Zingman, D. M. & Terzic, A. ATP-sensitive
745 potassium channels: metabolic sensing and cardioprotection. *J Appl Physiol (1985)*
746 **103**, 1888-1893 (2007). https://doi.org/10.1152/japplphysiol.00747.2007

747 93 Simons, M., Gordon, E. & Claesson-Welsh, L. Mechanisms and regulation of
748 endothelial VEGF receptor signalling. *Nat Rev Mol Cell Biol* **17**, 611-625 (2016).
749 https://doi.org/10.1038/nrm.2016.87

750 94 Chiplunkar, A. R. *et al.* The Kruppel-like factor 2 and Kruppel-like factor 4 genes
751 interact to maintain endothelial integrity in mouse embryonic vasculogenesis. *BMC*
752 *Dev Biol* **13**, 40 (2013). https://doi.org/10.1186/1471-213X-13-40

753 95 Zhang, P., Andrianakos, R., Yang, Y., Liu, C. & Lu, W. Kruppel-like factor 4 (Klf4)
754 prevents embryonic stem (ES) cell differentiation by regulating Nanog gene
755 expression. *J Biol Chem* **285**, 9180-9189 (2010).
756 https://doi.org/10.1074/jbc.M109.077958

757 96 Zhang, Y. *et al.* Kruppel-like factor 4 transcriptionally regulates TGF-beta1 and
758 contributes to cardiac myofibroblast differentiation. *PLoS One* **8**, e63424 (2013).
759 https://doi.org/10.1371/journal.pone.0063424

760 97 Stolzing, A. & Grune, T. Neuronal apoptotic bodies: phagocytosis and degradation by
761 primary microglial cells. *FASEB J* **18**, 743-745 (2004). https://doi.org/10.1096/fj.03-
762 0374fje

763 98 Zhang, H., Chen, X. & Sairam, M. R. Novel genes of visceral adiposity: identification of
764 mouse and human mesenteric estrogen-dependent adipose (MEDA)-4 gene and its
765 adipogenic function. *Endocrinology* **153**, 2665-2676 (2012).
766 https://doi.org/10.1210/en.2011-2008

767 99 Subramanian, S. V. & Nadal-Ginard, B. Early expression of the different isoforms of the
768 myocyte enhancer factor-2 (MEF2) protein in myogenic as well as non-myogenic cell
769 lineages during mouse embryogenesis. *Mech Dev* **57**, 103-112 (1996).
770 https://doi.org/10.1016/0925-4773(96)00542-4

771 100 Wang, L., Fan, C., Topol, S. E., Topol, E. J. & Wang, Q. Mutation of MEF2A in an
772 inherited disorder with features of coronary artery disease. *Science* **302**, 1578-1581
773 (2003). https://doi.org/10.1126/science.1088477

774 101 Bi, W., Drake, C. J. & Schwarz, J. J. The transcription factor MEF2C-null mouse exhibits
775 complex vascular malformations and reduced cardiac expression of angiopoietin 1 and
776 VEGF. *Dev Biol* **211**, 255-267 (1999). https://doi.org/10.1006/dbio.1999.9307

777 102 Lin, Q., Schwarz, J., Bucana, C. & Olson, E. N. Control of mouse cardiac morphogenesis
778 and myogenesis by transcription factor MEF2C. *Science* **276**, 1404-1407 (1997).
779 https://doi.org/10.1126/science.276.5317.1404

780 103 Kitajima, S., Takagi, A., Inoue, T. & Saga, Y. MesP1 and MesP2 are essential for the
781 development of cardiac mesoderm. *Development* **127**, 3215-3226 (2000).
782 https://doi.org/10.1242/dev.127.15.3215

783 104 Komata, M., Bando, M., Araki, H. & Shirahige, K. The direct binding of Mrc1, a
784 checkpoint mediator, to Mcm6, a replication helicase, is essential for the replication
785 checkpoint against methyl methanesulfonate-induced stress. *Mol Cell Biol* **29**, 5008-
786 5019 (2009). https://doi.org/10.1128/MCB.01934-08

787 105 Staines, K., Hunt, L. G., Young, J. R. & Butter, C. Evolution of an expanded mannose
788 receptor gene family. *PLoS One* **9**, e110330 (2014).
789 https://doi.org/10.1371/journal.pone.0110330

790 106 Roszer, T. Understanding the Mysterious M2 Macrophage through Activation Markers
791 and Effector Mechanisms. *Mediators Inflamm* **2015**, 816460 (2015).
792 https://doi.org/10.1155/2015/816460

793 107 Eon Kuek, L., Leffler, M., Mackay, G. A. & Hulett, M. D. The MS4A family: counting past
794 1, 2 and 3. *Immunol Cell Biol* **94**, 11-23 (2016). https://doi.org/10.1038/icb.2015.48

795 108 Martinez, F. O., Gordon, S., Locati, M. & Mantovani, A. Transcriptional profiling of the
796 human monocyte-to-macrophage differentiation and polarization: new molecules and

797 patterns of gene expression. *J Immunol* **177**, 7303-7311 (2006).
798 https://doi.org/10.4049/jimmunol.177.10.7303

799 109 England, J. & Loughna, S. Heavy and light roles: myosin in the morphogenesis of the
800 heart. *Cell Mol Life Sci* **70**, 1221-1239 (2013). https://doi.org/10.1007/s00018-012-
801 1131-1

802 110 Gawlik-Rzemieniewska, N. & Bednarek, I. The role of NANOG transcriptional factor in
803 the development of malignant phenotype of cancer cells. *Cancer Biol Ther* **17**, 1-10
804 (2016). https://doi.org/10.1080/15384047.2015.1121348

805 111 Ampofo, E., Schmitt, B. M., Menger, M. D. & Laschke, M. W. The regulatory
806 mechanisms of NG2/CSPG4 expression. *Cell Mol Biol Lett* **22**, 4 (2017).
807 https://doi.org/10.1186/s11658-017-0035-3

808 112 Fukushi, J., Makagiansar, I. T. & Stallcup, W. B. NG2 proteoglycan promotes
809 endothelial cell motility and angiogenesis via engagement of galectin-3 and
810 alpha3beta1 integrin. *Mol Biol Cell* **15**, 3580-3590 (2004).
811 https://doi.org/10.1091/mbc.e04-03-0236

812 113 Goretzki, L., Burg, M. A., Grako, K. A. & Stallcup, W. B. High-affinity binding of basic
813 fibroblast growth factor and platelet-derived growth factor-AA to the core protein of
814 the NG2 proteoglycan. *J Biol Chem* **274**, 16831-16837 (1999).
815 https://doi.org/10.1074/jbc.274.24.16831

816 114 Tanaka, M., Chen, Z., Bartunkova, S., Yamasaki, N. & Izumo, S. The cardiac homeobox
817 gene Csx/Nkx2.5 lies genetically upstream of multiple genes essential for heart
818 development. *Development* **126**, 1269-1280 (1999).
819 https://doi.org/10.1242/dev.126.6.1269

820 115 Song, W., Wang, H. & Wu, Q. Atrial natriuretic peptide in cardiovascular biology and
821 disease (NPPA). *Gene* **569**, 1-6 (2015). https://doi.org/10.1016/j.gene.2015.06.029

822 116 Pan, G. J., Chang, Z. Y., Scholer, H. R. & Pei, D. Stem cell pluripotency and transcription
823 factor Oct4. *Cell Res* **12**, 321-329 (2002). https://doi.org/10.1038/sj.cr.7290134

824 117 Zeineddine, D., Hammoud, A. A., Mortada, M. & Boeuf, H. The Oct4 protein: more than
825 a magic stemness marker. *Am J Stem Cells* **3**, 74-82 (2014).

826 118 El-Rass, S. *et al.* Disruption of pdgfra alters endocardial and myocardial fusion during
827 zebrafish cardiac assembly. *Biol Open* **6**, 348-357 (2017).
828 https://doi.org/10.1242/bio.021212

829 119 Horikawa, S. *et al.* PDGFRalpha plays a crucial role in connective tissue remodeling. *Sci*
830 *Rep* **5**, 17948 (2015). https://doi.org/10.1038/srep17948

831 120 Kim, J. *et al.* PDGF signaling is required for epicardial function and blood vessel
832 formation in regenerating zebrafish hearts. *Proc Natl Acad Sci U S A* **107**, 17206-17210
833 (2010). https://doi.org/10.1073/pnas.0915016107

834 121 Betsholtz, C. Insight into the physiological functions of PDGF through genetic studies
835 in mice. *Cytokine Growth Factor Rev* **15**, 215-228 (2004).
836 https://doi.org/10.1016/j.cytogfr.2004.03.005

837 122 Hsieh, P. C., Davis, M. E., Gannon, J., MacGillivray, C. & Lee, R. T. Controlled delivery
838 of PDGF-BB for myocardial protection using injectable self-assembling peptide
839 nanofibers. *J Clin Invest* **116**, 237-248 (2006). https://doi.org/10.1172/JCI25878

840 123 Peng, Y., Yan, S., Chen, D., Cui, X. & Jiao, K. Pdgfrb is a direct regulatory target of
841 TGFbeta signaling in atrioventricular cushion mesenchymal cells. *PLoS One* **12**,
842 e0175791 (2017). https://doi.org/10.1371/journal.pone.0175791

843 124 Van den Akker, N. M. *et al.* PDGF-B signaling is important for murine cardiac
844 development: its role in developing atrioventricular valves, coronaries, and cardiac
845 innervation. *Dev Dyn* **237**, 494-503 (2008). https://doi.org/10.1002/dvdy.21436

846 125 Wilkinson, S., O'Prey, J., Fricker, M. & Ryan, K. M. Hypoxia-selective macroautophagy
847 and cell survival signaled by autocrine PDGFR activity. *Genes Dev* **23**, 1283-1288
848 (2009). https://doi.org/10.1101/gad.521709

849 126 Yue, Z. *et al.* PDGFR-beta Signaling Regulates Cardiomyocyte Proliferation and
850 Myocardial Regeneration. *Cell Rep* **28**, 966-978 e964 (2019).
851 https://doi.org/10.1016/j.celrep.2019.06.065

852 127 Grossi, S. *et al.* Molecular genetic analysis of the PLP1 gene in 38 families with PLP1-
853 related disorders: identification and functional characterization of 11 novel PLP1
854 mutations. *Orphanet J Rare Dis* **6**, 40 (2011). https://doi.org/10.1186/1750-1172-6-40

855 128 Alquraini, A. *et al.* The autocrine role of proteoglycan-4 (PRG4) in modulating
856 osteoarthritic synoviocyte proliferation and expression of matrix degrading enzymes.
857 *Arthritis Res Ther* **19**, 89 (2017). https://doi.org/10.1186/s13075-017-1301-5

858 129 Han, L., Grodzinsky, A. J. & Ortiz, C. Nanomechanics of the Cartilage Extracellular
859 Matrix. *Annu Rev Mater Res* **41**, 133-168 (2011). https://doi.org/10.1146/annurev-
860 matsci-062910-100431

861 130 Dawes, R. *et al.* Combinations of CD45 isoforms are crucial for immune function and
862 disease. *J Immunol* **176**, 3417-3425 (2006).
863 https://doi.org/10.4049/jimmunol.176.6.3417

864 131 Hermiston, M. L., Xu, Z. & Weiss, A. CD45: a critical regulator of signaling thresholds in
865 immune cells. *Annu Rev Immunol* **21**, 107-137 (2003).
866 https://doi.org/10.1146/annurev.immunol.21.120601.140946

867 132 Nakano, A., Harada, T., Morikawa, S. & Kato, Y. Expression of leukocyte common
868 antigen (CD45) on various human leukemia/lymphoma cell lines. *Acta Pathol Jpn* **40**,
869 107-115 (1990). https://doi.org/10.1111/j.1440-1827.1990.tb01549.x

870 133 Batts, T. D. *et al.* Stem cell antigen-1 (sca-1) regulates mammary tumor development
871 and cell migration. *PLoS One* **6**, e27841 (2011).
872 https://doi.org/10.1371/journal.pone.0027841

873 134 Bradfute, S. B., Graubert, T. A. & Goodell, M. A. Roles of Sca-1 in hematopoietic
874 stem/progenitor cell function. *Exp Hematol* **33**, 836-843 (2005).
875 https://doi.org/10.1016/j.exphem.2005.04.001

876 135 Ito, C. Y., Li, C. Y., Bernstein, A., Dick, J. E. & Stanford, W. L. Hematopoietic stem cell
877 and progenitor defects in Sca-1/Ly-6A-null mice. *Blood* **101**, 517-523 (2003).
878 https://doi.org/10.1182/blood-2002-06-1918

879 136 Upadhyay, G. *et al.* Stem cell antigen-1 enhances tumorigenicity by disruption of
880 growth differentiation factor-10 (GDF10)-dependent TGF-beta signaling. *Proc Natl*
881 *Acad Sci U S A* **108**, 7820-7825 (2011). https://doi.org/10.1073/pnas.1103441108

882 137 Tandon, P., Miteva, Y. V., Kuchenbrod, L. M., Cristea, I. M. & Conlon, F. L. Tcf21
883 regulates the specification and maturation of proepicardial cells. *Development* **140**,
884 2409-2421 (2013). https://doi.org/10.1242/dev.093385

885 138 Mattson, M. P., Fu, W. & Zhang, P. Emerging roles for telomerase in regulating cell
886 differentiation and survival: a neuroscientist's perspective. *Mech Ageing Dev* **122**, 659-
887 671 (2001). https://doi.org/10.1016/s0047-6374(01)00221-4

888 139 Yuan, X., Larsson, C. & Xu, D. Mechanisms underlying the activation of TERT
889 transcription and telomerase activity in human cancer: old actors and new players.
890 *Oncogene* **38**, 6172-6183 (2019). https://doi.org/10.1038/s41388-019-0872-9

891 140 Peyvandi, F., Garagiola, I. & Baronciani, L. Role of von Willebrand factor in the
892 haemostasis. *Blood Transfus* **9 Suppl 2**, s3-8 (2011).
893 https://doi.org/10.2450/2011.002S

894 141 Lu, D. *et al.* WIF1 causes dysfunction of heart in transgenic mice. *Transgenic Res* **22**,
895 1179-1189 (2013). https://doi.org/10.1007/s11248-013-9738-z

896 142 Smits, A. M., Dronkers, E. & Goumans, M. J. The epicardium as a source of multipotent
897 adult cardiac progenitor cells: Their origin, role and fate. *Pharmacol Res* **127**, 129-140
898 (2018). https://doi.org/10.1016/j.phrs.2017.07.020

899 143 Zhao, L. *et al.* Notch signaling regulates cardiomyocyte proliferation during zebrafish
900 heart regeneration. *Proc Natl Acad Sci U S A* **111**, 1403-1408 (2014).
901 https://doi.org/10.1073/pnas.1311705111

902 144 Schildmeyer, L. A. *et al.* Impaired vascular contractility and blood pressure
903 homeostasis in the smooth muscle alpha-actin null mouse. *FASEB J* **14**, 2213-2220
904 (2000). https://doi.org/10.1096/fj.99-0927com

905